Dielectric Studies of Some Synthetic Poly(α-amino acid)s and Collagen

Naoki SASAKI

DISSERTATION

FOR

THE DEGREE OF DOCTOR OF SCIENCE

FACULTY OF SCIENCE

HOKKAIDO UNIVERSITY

SAPPORO, JAPAN

December 1979

CONTENTS

ABSTRACT

Molecular motions of some poly(α-amino acid)s and collagen with absorbed water were investigated by the method of dielectric measurements. Polymers studied are poly(γ-n-alkyl L-glutamate)s(PnALG)s, poly(γ-monosubstituted benzyl D-glutamate)s, poly(ε-N-benzyloxycarbonyl-L-lysine) (PCLL), and related poly(α-amino acid)s. Collagen is bovine Achilles tendon.

Each sample of poly(α-amino acid)s exhibits a dielectric dispersion in the vicinity of room temperature due to side-chain motions. The time—temperature superposition principle was found to be applicable to obtain the master curve for all samples.

The dispersion temperatures of PnALGs were found to decrease monotonously with increasing the number of carbons in the side-chain alkyl group. It was found that the distribution of the relaxation time broadens with the decrease in the number of carbons in the side-chain alkyl group. These results were discussed in terms of the two-phase model, in which the rigid α-helical backbone chain is embedded in flexible side-chain region.

The dielectric dispersion temperature (the temperature of maximum loss) is influenced by the introduction of substituents into the side chain of poly(α-amino acid). Among three monochlorosubstituted PBDGs, poly[γ-(p-chlorobenzyl) D-glutamate](p-ClPBDG) showed the highest dispersion

temperature. Among p-monosubstituted PBDGs, poly[γ-(p-nitrobenzyl) D-glutamate] showed the highest dispersion temperature. This polymer has the side chain with the largest dipole moment among three p-sbstituents studied here. The results were explained in terms of the restriction to motions caused by dipole-dipole interaction among dipoles in the side-chain region. Racemic mixtures of p-ClPBDG and p-ClPBLG showed no evidence of the first order solid-solid phase transition, which has been reported to be observed for racemic mixtures of PBDG and PBLG.

The dielectric dispersion temperatures of PCLL, a mixture of PCLL and PBDG(PCLL + PBDG), and copolymers of CLL-residue and BLG-residue(PCLBG) were higher than those of PBLG and PMLG. A strong interaction was assumed to exist between side chains of PCLL. Infrared spectroscopic measurements revealed that urethane groups in CLL-side chains are hydrogen-bonded. Fraction of hydrogen bonds of side chain of PCLL, PCLL + PBDG, and PCLBG were estimated from infrared spectroscopy. The results of dielectric measurements were interpreted in terms of the hydrogen bond.

The dielectric constant of native collagen with absorbed water shows a sharp increase with increasing water content beyond a certain value and becomes enormous to overgrow the value of pure water. In order to correlate the dielectric behavior with the structural properties of collagen, X-ray diffraction measurements were performed. The X-ray study showed that the spacing of neighboring tropocollagens increases with increasing water content in

a region where the sharp increase of the dielectric constant occurs. Thus, the sharp increase of the dielectric constant was found to occur in the hydration stage where water molecules pack into the inter-tropocollagen region. The behavior of the dielectric constant as a function of water content was discussed in terms of the property of water crust surrounding tropocollagens which may vary with the increase in thickness of the crust of water.

ACKNOWLEDGEMENTS

The research works described in this thesis have been made at Polymer Physics Laboratory, Department of Polymer Science, Faculty of Science, Hokkaido University.

I would like to express my gratitude for inspiring guidance and many fruitful suggestions of Professor K. Hikichi. To Professor A. Tsutsumi, I am grateful for his helpful advises about both experimental and theoretical approaches of this work. Grateful acknowledgement is also made to Professor M. Kaneko for his continual encouragements throughout this work. I thank other members of Polymer Physics Laboratory. I am indebted to Dr. N. Matsushima for many philosophical discussions, to Dr. Y. Yamashita for his practical advices, to Dr. T. Hiraoki for taking NMR spectra, to M. M. Osanai and M. S. Shiwa for advices about X-ray measurements, to Mr. H. Shimodate for his cooperation, to M. S. Yagihara and M. M. Tokita for helpful comments, to Miss T. Ohno and Miss C. Tasai for secretarial assiatance.

I am also grateful to Professor M. Yoneyama for advises about infrared spectroscopic measurements, to Professor Y. Satō of Iwate University for experimental advices, to Professor M. Hatano and Dr. Y. Konishi of Tohoku University for kindly providing monosubstituted PBDGs.

Naoki Sasaki

December, 1979

ABBREVIATIONS

PnALG	Poly(γ-n-alkyl L-glutamate)
PMLG	Poly(γ-methyl L-glutamate)
PELG	Poly(γ-ethyl L-glutamate)
PnPLG	Poly(γ-n-propyl L-glutamate)
PnBtLG	Poly(γ-n-butyl L-glutamate)
PnAmLG	Poly(γ-n-amyl L-glutamate)
PnHxLG	Poly(γ-n-hexyl L-glutamate)
o-ClPBDG	Poly[γ-(o-chlorobenzyl) D-glutamate]
m-ClPBDG	Poly[γ-(m-chlorobenzyl) D-glutamate]
p-ClPBDG	Poly[γ-(p-chlorobenzyl) D-glutamate]
p-NPBDG	Poly[γ-(p-nitrobenzyl) D-glutamate]
p-MePBDG	Poly[γ-(p-methylbenzyl) D-glutamate]
p-ClPBDG + p-ClPBLG	Racemic mixture of p-ClPBDG and p-ClPBLG
PCLL	Poly(ε-N-benzyloxycarbonyl-L-lysine)
PCLL + PBDG	Mixture of PCLL and PBDG
PCLBG	Copolymer of ε-N-benzyloxycarbonyl-L-lysine and γ-benzyl L-glutamate

CHAPTER I

INTRODUCTION

For many years, poly(α-amino acid) has been used as a simple model compound in the theoretical and experimental studies of the interaction which plays an important role to determine the three dimensional conformation of proteins. Major parts of such studies on poly(α-amino acid), hitherto, have been devoted to the investigation on the conformation in solution in order to understand the structure and function of globular proteins. On the other hand, there is a dearth of information available for the solid state nature of poly(α-amino acid), which may produce a molecular aggregation model about the self assembly of fibrous proteins.

The author's interest has been focused on the study of solid state properties of some synthetic polypeptides and of fibrous proteins. In order to understand the properties of the solid state materials, it seems to be one of the fruitful approaches to investigate the molecular motion.

Since molecular motions of poly(α-amino acid)s in the solid state were first investigated,[1] a considerable body of experimental data has been accumulated by the methods of nuclear magnetic,[2-4] dynamic mechanical,[4-8] and dielectric measurements.[4, 9-14] According to these results, even in the solid state long side chains of the α-helical poly(α-amino acid) undergo considerable motions while the

α-helical backbone chain remains rigid. Side-chain motions have been found to occur in solid films of poly(γ-benzyl L-glutamate)(PBLG) and poly(γ-methyl L-glutamate)(PMLG). These side-chain motions have characteristic features which are reminiscent of a glass transition, indicating that the side-chain region of these poly(α-amino acid)s is quite similar to the glass-forming liquid.[4,6]

These results indicate that some properties of the α-helical poly(α-amino acid) having the long side chain could be explained if we regard it as a composite system of two independent parts, the side chain and the α-helical backbone chain.

The coaxial two-phase model which consists of the rigid α-helical core and the flexible side chain surrounding it has been proposed to account for the solution properties of PBLG[15] and for the temperature dependence of the X-ray diffraction intensity of lateral reflections for PMLG and PBLG in the solid state.[16] The two-phase model has also been adopted to explain the thermal behavior of some α-helical poly(α-amino acid)s having the long side chain.[6]

In this thesis, the dielectric properties of α-helical poly(α-amino acid) in the solid state are examined in the light of the two-phase model. The second chapter deals with dielectric measurements which are carried out to make certain of the general applicability of the two-phase model to the poly(α-amino acid) in the solid state. According to the model, interactions in the solid state α-helical poly(α-amino acid) may be divided into the two species;

the interaction in the side-chain region and that between the backbone and the side-chain region.

In Chapter III and IV, interactions in the side-chain region are investigated as constraints affecting the side-chain motion. In Chapter III, the effects upon the molecular motion of the introduction of the substituents into the side chain are discussed. In Chapter IV, the strong restriction on the molecular motion of the side chain observed in poly(ε-N-benzyloxycarbonyl-L-lysine) is interpreted in terms of the hydrogen bonding in the side-chain urethane group which has been observed for this polymer in helicogenical solutions.[17]

In Chapter V, the dielectric properties of native collagen with absorbed water are examined. The results will be discussed on the basis of the structure of the hydration. Concluding remarks are presented in Chapter VI.

REFERENCES

1. J. A. E. Kail, J. A. Sauer, and A. E. Woodward, J. Phys. Chem., 66, 1292 (1963).
2. K. Hikichi, J. Phys. Soc. Jpn., 19, 2169 (1964).
3. A. Tsutsumi, Jpn. J. Appl. Phys., 9, 2225 (1970).
4. A. Tsutsumi, K. Hikichi, T. Takahashi, Y. Yamashita, N. Matsushima, M. Kanke, and M. Kaneko, J. Macromol. Sci.-Phys., B8, 413 (1973).
5. R. G. Saba, J. A. Sauer, and A. E. Woodward, J. Polym. Sci., Part A, 1, 1843 (1963).
6. Y. Yamashita, A. Tsutsumi, K. Hikichi, and M. Kaneko, Polym. J., 8, 114 (1975).
7. Y. Yamashita, A. Tsutsumi, K. Hikichi, and M. Kaneko, Polym. J., 11, 241 (1979).
8. T. Kajiyama, M. Kuroishi, and M. Takayanagi, J. Macromol. Sci.-Phys., B11, 195 (1975).
9. K. Hikichi, K. Saito, M. Kaneko, and J. Furuichi, J. Phys. Soc. Jpn., 19, 557 (1964).
10. S. Makino, K. Kamashima, S. Kubota, and S. Sugai., Jpn. J. Appl. Phys., 3, 55 (1964).
11. S. Sugai, K. Kamashima, S. Makino, and J. Noguchi, J. Polym. Sci., Part A-2, 4, 183 (1966).
12. A. Tsutsumi, K. Hikichi, M. Mitsumaki, M. Kaneko, and J. Furuichi, J. Phys. Soc. Jpn., 22, 1120 (1967).
13. T. Takahashi, A. Tsutsumi, K. Hikichi, and M. Kaneko, Macromolecules, 7, 806 (1974).

14. N. Sasaki, Y. Yamashita, A. Tsutsumi, and K. Hikichi, Polym. J., 10, 207 (1978).

15. P. J. Flory and W. J. Leonard, Jr., J. Am. Chem. Soc., 87, 2102 (1965).

16. N. Matsushima and K. Hikichi, Polym. J., 10, 437 (1978).

17. M. Hatano and M. Yoneyama, J. Am. Chem. Soc., 92, 1392 (1970).

CHAPTER II

DIELECTRIC MEASUREMENTS OF POLY(γ-n-ALKYL L-GLUTAMATE)S IN THE SOLID STATE AS A CHECK OF THE APPLICABILITY OF THE TWO-PHASE MODEL

It may be considered from the view point of the two-phase model that the α-helical poly(α-amino acid) having flexible side chains has a similar structure as the conventional semicrystalline polymer composed of both amorphous and crystalline regions or the amorphous polymer containing the rigid filler. That is, the side chain of poly(α-amino acid) corresponds to the amorphous region of semi-crystalline polymer and the α-helical backbone chain to the crystalline region or filler. Thus, the α-helical poly(α-amino acid) having long side chain may behave in a similar way as the semi-crystalline polymer with a small degree of crystallinity and the filled amorphous polymer having a small fraction of fillers. The increase in the length of the side chain of the α-helical poly(α-amino acid) may be regarded as the decrease in the degree of crystallinity of semi-crystalline polymer and in the fraction of fillers of the filled amorphous polymer.[1]

In this chapter, in order to examine the applicability of the two-phase model to the α-helical poly(α-amino acid) in the solid state, dielectric measurements were performed for six poly(γ-n-alkyl L-glutamate)s(PnALG)s which have the varying number of carbons in the alkyl group at the end of

the side chain.

The effects of the variation of the side-chain length upon the solid state properties are examined in a similar way as the semi-crystalline polymers had been examined as a function of the degree of crystallinity.

Polymers used in this work and abbreviations are as follows: poly(γ-methyl L-glutamate)(PMLG), poly(γ-ethyl L-glutamate)(PELG), poly(γ-n-propyl L-glutamate)(PnPLG), poly(γ-n-butyl L-glutamate)(PnBtLG), poly(γ-n-amyl L-glutamate)(PnAmLG), and poly(γ-n-hexyl L-glutamate)(PnHxLG).

II-1. EXPERIMENTAL

Various PnALGs were synthesized by the ester exchange reaction of PMLG(Ajicoat A-2000) with corresponding alcohols. The degree of substitution was checked by proton NMR spectra. For all samples, the exchange reaction was almost completely achieved.

Films of all samples for dielectric measurements were prepared by casting from concentrated chloroform solution on a glass plate at room temperature. Infrared spectra of films of PnALG exhibited amide V band at about 615-620 cm^{-1}, indicating that in the film the backbone chain of PnALG is in the α-helical form.

Silver electrodes were vacuum-deposited on both surfaces of film to assure complete electric contact. Each film was set in the measuring cell and evacuated at a temperature of some 120°C until the dielectric constant remains unchanged.

Dielectric constant and loss factor were measured by an Ando Denki TR-1C bridge with a lock-in amplifier LI-573 of NF Circuit Design Block Co., Ltd. and an Ando Denki WBG-5 oscillator. Measurements were made over a frequency range from 30Hz to 300kHz and a temperature range from -150 to 100°C.

II-2. RESULTS AND DISCUSSION

Figures 2.1(a) and (b) show the temperature dependence of tanδ measured at a frequency of 1kHz for PMLG, PELG, and PnPLG and for PnBtLG, PnAmLG, and PnHxLG, respectively. Each sample shows two dielectric dispersions, the one located in the vicinity of 0°C and the other located at about -150°C. For PMLG the dispersion observed in the vicinity of 0°C has been considered to be caused by the onset of the micro-Brownian motion of the whole side chain,[2,3] and the dispersion observed at about -150°C is due to the oscillational motion of the side chain on a small scale.[2,4,5] Dielectric dispersions observed for other samples will be assigned to the same origins as for PMLG.

The temperature region of the dispersion near 0°C seemed to shift to lower temperatures with increasing the side-chain length, while the dispersion at about -150°C remained unchanged for all samples measured. In this paper, we will discuss only the dispersion near 0°C.

For all samples measured, the time-temperature superposition principle was found to be applicable to obtain the master curve. Figure 2.2 shows the shift factor b_T, used in the superposition procedure, as a function of temperature. In this figure, the full curve represents the universal WLF-equation[6]

$$\log b_T = \frac{-8.86\ (T - T_S)}{101.6 + (T - T_S)} \qquad \text{(II-1)}$$

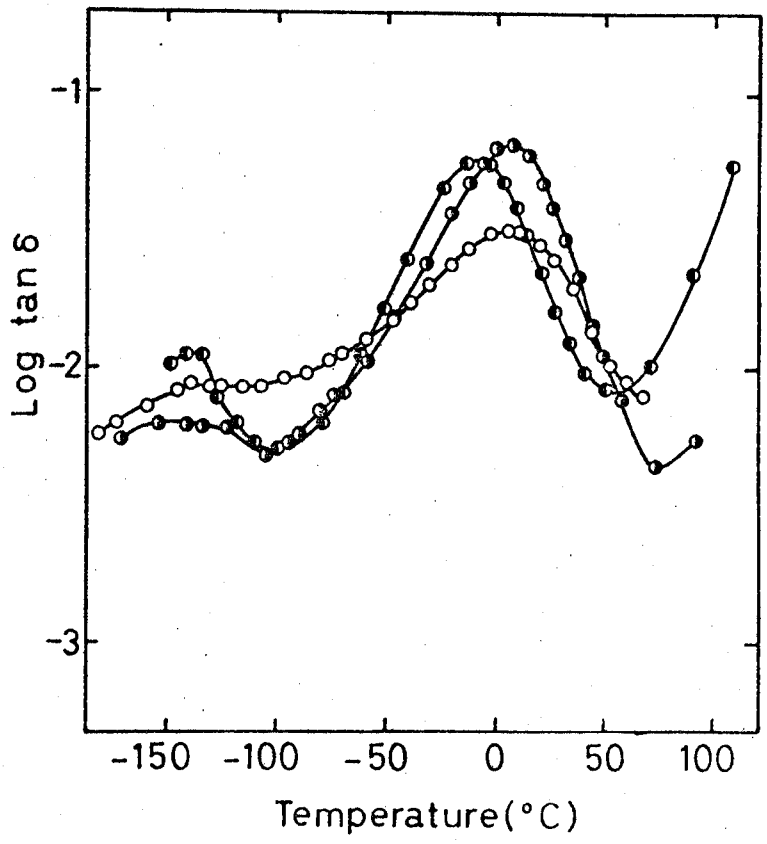

Figure 2.1 (a). Temperature dependence of tanδ for PMLG(○), PELG(◑), and PnPLG(◐) measured at a frequency of 1kHz.

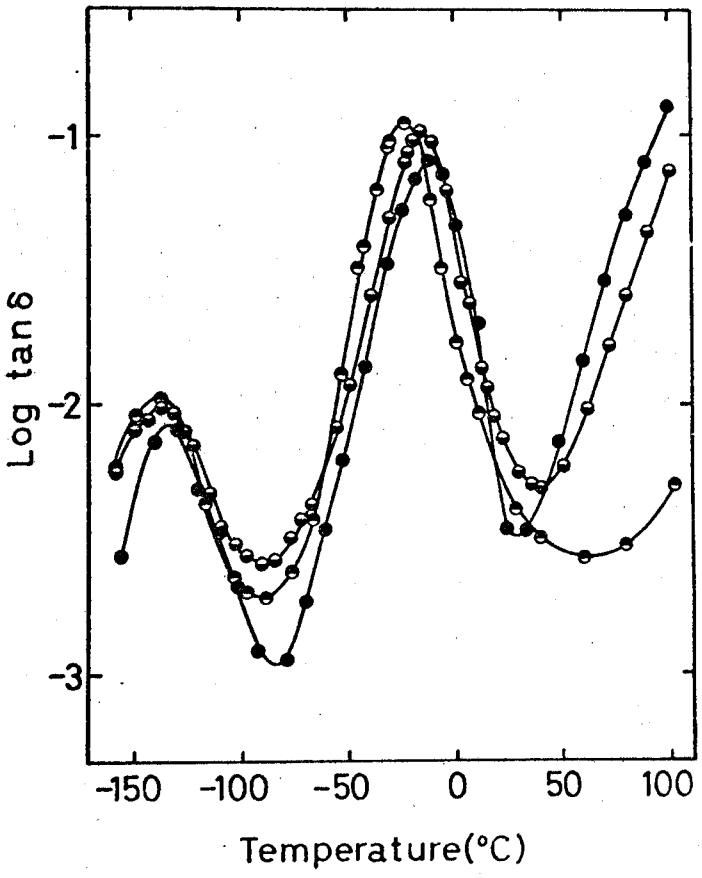

Figure 2.1 (b). Temperature dependence of tanδ for PnBtLG(●), PnAmLG(◒), and PnHxLG(◓) measured at a frequency of 1kHz.

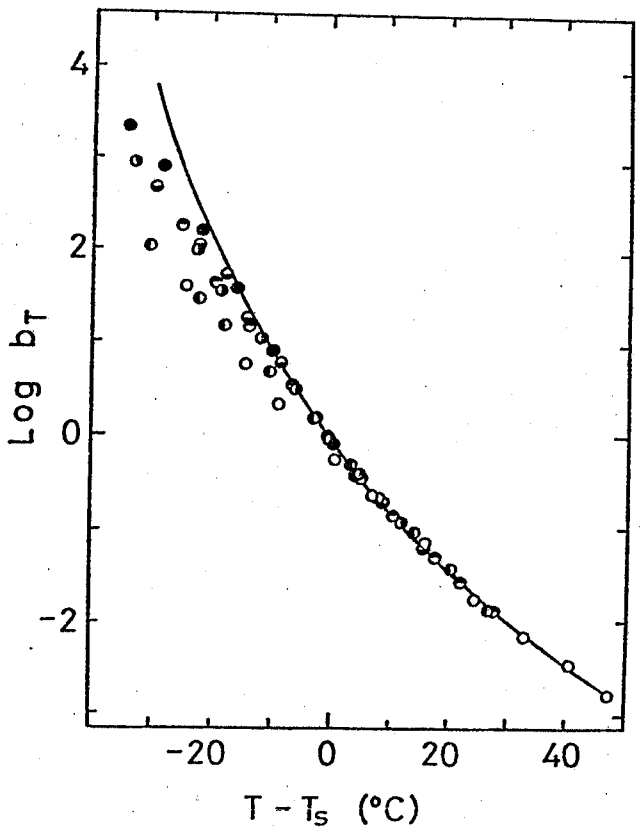

Figure 2.2. b_T plotted against temperature for PMLG (○), PELG(◑), PnPLG(◐), PnBtLG(●), PnAmLG(◒), and PnHxLG(◓).

For each sample, the temperature dependence of b_T is found to be well expressed by the WLF-equation, if an appropriate choice of the standard temperature T_s is made.

In Figure 2.3, the temperature dependence of the relaxation strength $\Delta\varepsilon$ is shown. The relaxation strength was determined by the Cole-Cole plot. For all samples, $\Delta\varepsilon$ decreases with increasing temperature.

These behaviors of both b_T and $\Delta\varepsilon$ against temperature indicate that the dispersions observed near 0°C for all samples studied have a resemblance to the primary dispersion related to the glass transition of the amorphous polymer, as in the case of PMLG and other poly(glutamate)s.[2,3]

Figure 2.4 shows the dispersion temperature T_{max}, defined as the temperature of maximum tan δ, as a function of the number of carbons of the alkyl group in the side chain. As is expected by the glimpse of Figure 2.4, T_{max} is found to decrease with increasing the side-chain length. This suggests that the side-chain motion is released at lower temperatures as the number of carbons in the alkyl group increases.

The finding that T_{max} decreases with an increase in the number of carbons of the side-chain alkyl group seems to have good correlation with the observations that T_{max} of the primary dispersion decreases with a decrease in the degree of crystallinity for the semi-crystalline polymers or with the decrease in the fraction of fillers for the filled amorphous polymer.[7,8,9] The decrease in T_{max} with increasing the side-chain length suggests a decrease

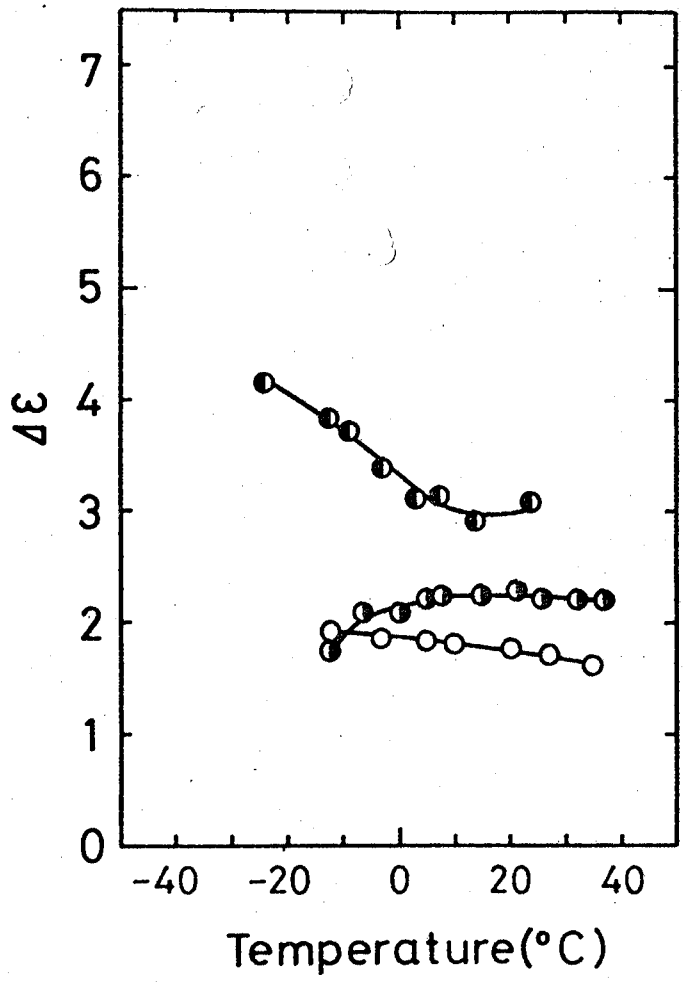

Figure 2.3 (a). The relaxation strength $\Delta\varepsilon$ plotted against temperature for PMLG(○), PELG(◑), and PnPLG(◐).

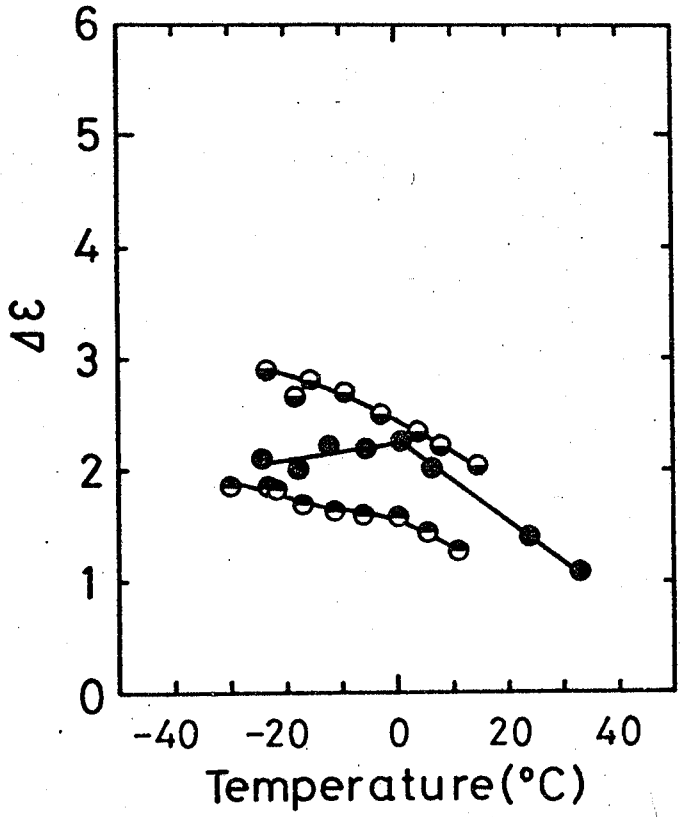

Figure 2.3 (b). The relaxation strength Δε plotted against temperature for PnBtLG(●), PnAmLG(◒), and PnHxLG(◓).

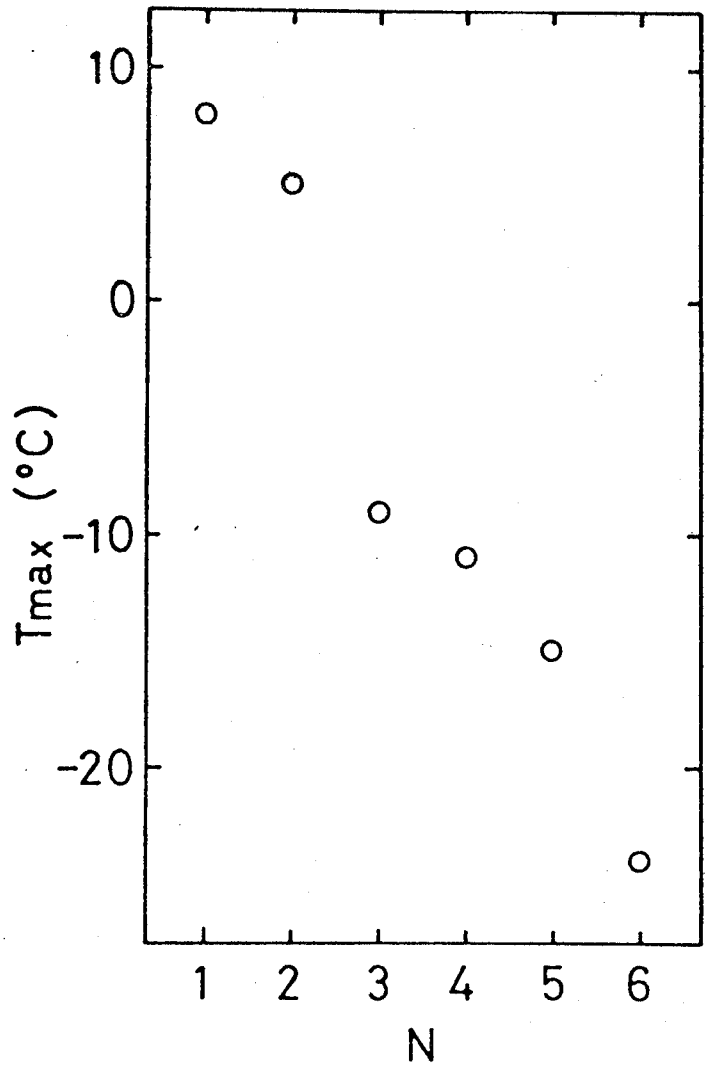

Figure 2.4. The dispersion temperature T_{max} as a function of the number of carbons in the side-chain alkyl group, N.

in the interaction between the crystalline region(corresponding to the α-helical backbone chain) and the amorphous region(the side chain).

In Figure 2.5, the master curves of the reduced loss factor ε''_R for PnALGs are compared, ε''_R being defined as the loss factor ε" divided by Δε. Here, the reduced loss factor is normalized with respect to its maximum value ε''_{Rmax} and the reduced frequency is normalized with respect to the value at which the maximum reduced loss occurs. The reduced frequency is defined as fb_T. Experimental points were omitted for the sake of clarity. The slope on the higher-frequency side of the master curve of the loss factor represents approximately the slope in the wedge-type region of the retardation spectrum except for sign. In the retardation spectrum, the slope of 1/2 has been predicted based on Rouse's bead-spring model, which well represents the characteristic features of the relaxation behavior of many amorphous polymers. In this figure, the line A corresponds to the slope of 1/2 in the retardation spectrum.

It has been known that the distribution of the relaxation time of the primary dispersion of the semi-crystalline polymer or the filled amorphous polymer is broadened by the increase in the degree of crystallinity or the filler content.[8,9] It is apparent from Figure 2.5 that PMLG shows the broadest distribution of the relaxation time, and that the slope on the higher-frequency side of the master curve approaches the slope A as the side-chain

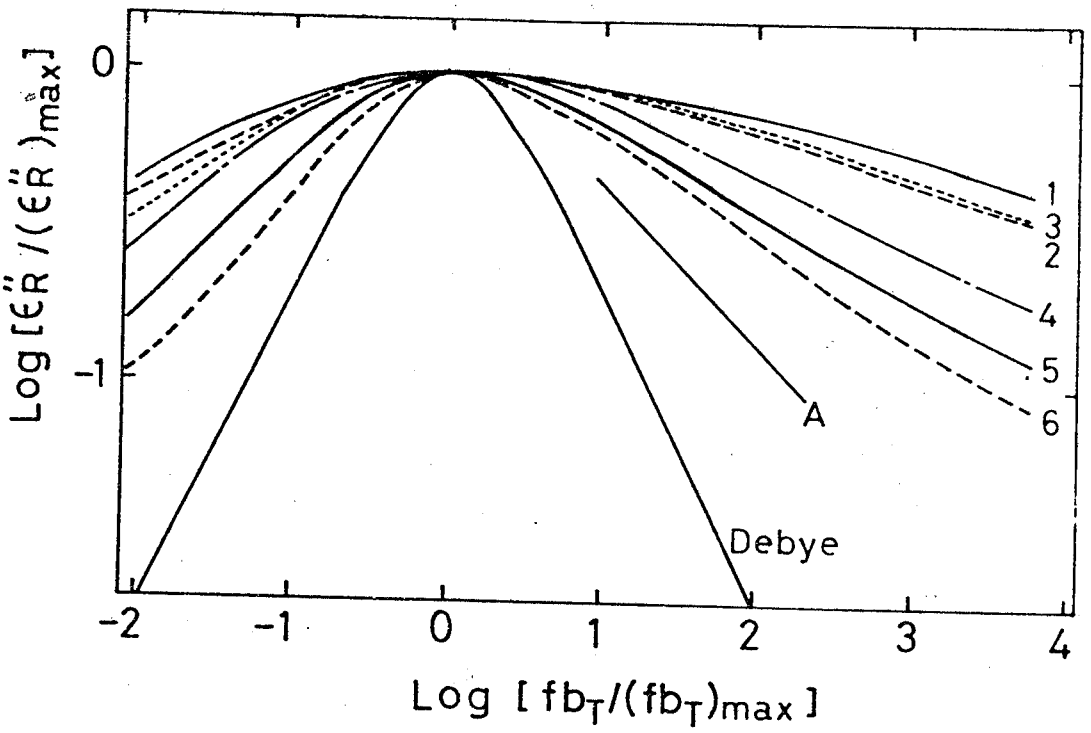

Figure 2.5. Comparison of master curves of the reduced loss factor ε''_R / ε''_{Rmax}. Abscissa is the logarithm of the reduced frequency normalized by the value at which the maximum loss occurs. Figures in the diagram represent the number of carbons in the side-chain alkyl group of PnALG. The slope of line A corresponds to that theoretically predicted for the amorphous polymers.

length increases.

Ishida et al. examined the primary dielectric dispersion of the semi-crystalline polymers as a function of the degree of crystallinity[10] and discussed their results in the light of Kirkwood's sech-law,[11]

$$\varepsilon''_R / \varepsilon''_{Rmax} = \mathrm{sech}[\ \bar{\alpha}\ \ln\ (\ f / f_{max}\ )] \qquad \text{(II-2)}$$

where $\bar{\alpha}$ is a parameter representing the breadth of the distribution of the relaxation time, f is the frequency, and f_{max} is the frequency at which the loss maximum occurs. $\bar{\alpha} = 1$ corresponds to Debye's dispersion: the smaller the value of $\bar{\alpha}$, the broader the master curve. They found that $\bar{\alpha}$ decreases monotonously with the increase in the degree of crystallinity.

Kirkwood's law is simply rewritten as

$$\cosh^{-1}(\ \varepsilon''_{Rmax} / \varepsilon''_R\ ) = \bar{\alpha}\ \ln\ (\ f / f_{max}\ ) \qquad \text{(II-3)}$$

In Figure 2.6 is shown the left hand side of eq II-3 as a function of the logarithm of the reduced frequency in the higher-frequency region. In the region under discussion of the master curve, Kirkwood's sech-law holds well, showing the linear relation between the both sides of eq II-3. The slope of the plot in the figure gives the value of the parameter $\bar{\alpha}$.

In Figure 2.7, the parameter $\bar{\alpha}$ is plotted against the length of the side chain. It is clearly observed that the

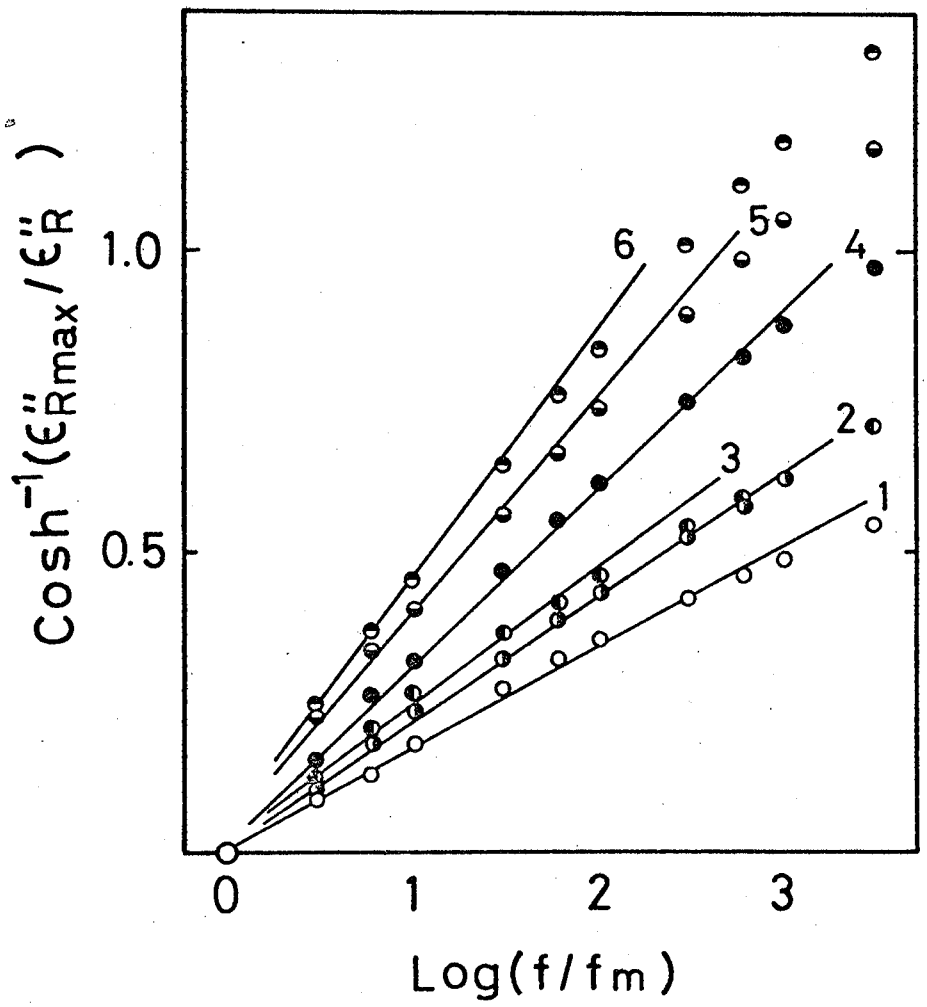

Figure 2.6. The left hand side of eq II-3 $\cosh^{-1}(\varepsilon''_{Rmax} / \varepsilon''_{R})$ plotted against the logarithm of the reduced frequency. Figures in the diagram represent the number of carbons in the side-chain alkyl group of PnALG.

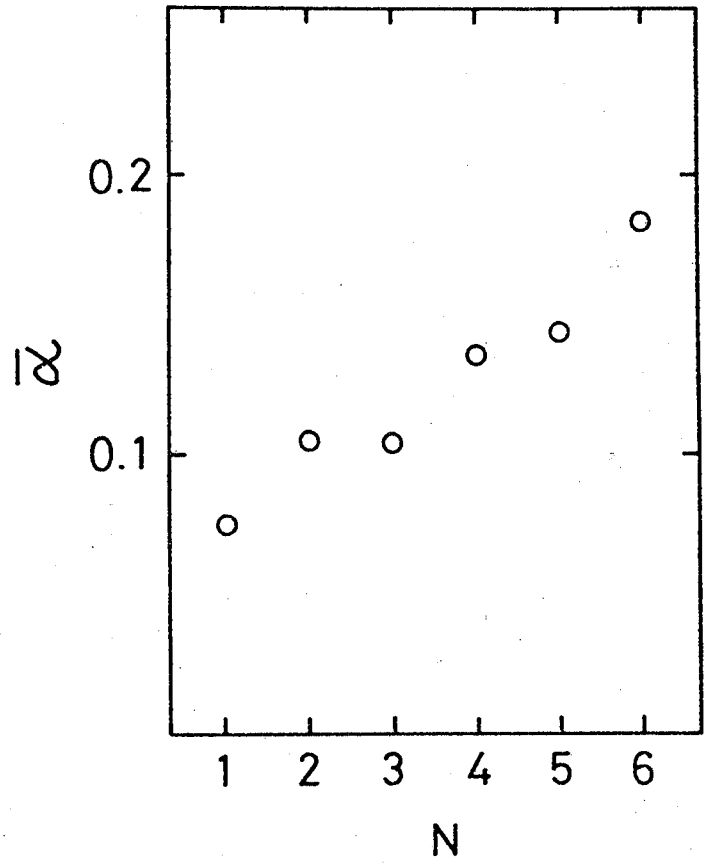

Figure 2.7. $\bar{\alpha}$ as a function of the number of carbons of the alkyl group in the side chain of PnALG, N.

value of $\bar{\alpha}$ increases as the side-chain length increases. These results accord well with those of Ishida's work, if the increase in the side-chain length is regarded as equivalent to the decrease in the degree of crystallinity.

The fact that variations in T_{max} and in $\bar{\alpha}$ of PnALGs with the side-chain length have a good correlation with those for the semi-crystalline polymer and/or the filled amorphous polymer suggests that it is reasonable to explain the dielectric behavior at least in terms of the two-phase model, if the change in the side-chain length is assumed to correspond to the variation in the degree of crystallinity or of the fraction of fillers.

In conclusion, the present dielectric studies on various PnALGs indicate that the two-phase model is, at least approximately, applicable to the structure of the α-helical poly(α-amino acid) having a flexible side chain in the solid state.

REFERENCES

1. Y. Yokomori, Y. Uematsu, and I. Uematsu, Rep. Prog. Polym. Phys. Jpn., 15, 633 (1972).
2. A. Tsutsumi, K. Hikichi, T. Takahashi, Y. Yamashita, N. Matsushima, M. Kanke, and M. Kaneko, J. Macromol. Sci.-Phys., B8, 413 (1973).
3. Y. Yamashita, A. Tsutsumi, K. Hikichi, and M. Kaneko, Polym. J., 8, 114 (1975).
4. K. Yamafuji, J. Phys. Soc. Jpn., 15, 633 (1960).
5. R. Hayakawa and Y. Wada, J. Polym. Sci. Polym. Phys. Ed., 12, 2119 (1974).
6. M. L. Williams, R. F. Landel, and J. D. Ferry, J. Am. Chem. Soc., 77, 3701 (1955).
7. K. H. Illers and H. Breuer, J. Colloid Sci., 18, 1 (1963).
8. R. F. Landel, Trans. Soc. Rheology, 2, 53 (1958).
9. J. D. Ferry, " Viscoelastic Properties of polymers " John Wiley & Sons, New York (1960).
10. Y. Ishida, K. Yamafuji, H. Ito, and M. Takayanagi, Kolloid-Z. u. Z. Polymere, 184, 97 (1962).
11. R. M. Fuoss and J. G. Kirkwood, J. Am. Chem. Soc., 63, 358 (1941).

CHAPTER III

DIELECTRIC STUDIES OF INFLUENCES OF SUBSTITUENT GROUPS UPON SIDE-CHAIN MOTIONS OF POLY(α-AMINO ACID)

According to the results in the preceding chapter, it may be suggested that interactions in the solid-state α-helical poly(α-amino acid) are able to be divided into the following two kinds; the backbone chain—side chain interaction and the side chain—side chain interaction. Both of these interactions depend on the chemical nature of the side chain.

It has been reported that in a series of poly(γ-monosubstituted benzyl D-glutamate)s in which a substituent is introduced into the phenyl ring at the end of the side chain of poly(γ-benzyl D-glutamate), properties markedly depend on the species and the position of the substituent.[1-3] It has been also reported that the different position of the substitution affects the conformation of the α-helical backbone.[4,5] Though qualitatively, the dependence of the helical structure and its stability on the species of the side chain has been explained in terms of side chain—side chain and side chain—backbone chain interactions.[6]

The discussion of the present chapter is focused on the side chain—side chain interaction. We examined the effects of the substitution to the benzyl group of PBDG on side-chain motions.

Dielectric and broad-line NMR measurements were per-

formed to observe molecular motions for the following seven samples of poly(γ-monosubstituted benzyl glutamate)s; poly[γ-(o-chlorobenzyl) D-glutamate](o-ClPBDG), poly[γ-(m-chlorobenzyl) D-glutamate](m-ClPBDG), poly[γ-(p-chlorobenzyl) D-glutamate](p-ClPBDG), poly[γ-(p-chlorobenzyl) L-glutamate](p-ClPBLG), poly[γ-(p-nitrobenzyl) D-glutamate](p-NPBDG), poly[γ-(p-methylbenzyl) D-glutamate](p-MePBDG), and the racemic mixture of p-ClPBDG and p-ClPBLG(p-ClPBDG + p-Cl PBLG). In particular, p-ClPBDG + p-ClPBLG was investigated from the point of view of phenyl ring stacking since such a stacking has been reported to occur for a racemic mixture of PBLG and PBDG.[7-12]

III-1. EXPERIMENTAL

All samples except for two polymers of p-ClPBDG and p-ClPBLG were prepared by the ester exchanging reaction of PMDG with corresponding alcohols.[3, 13] The degree of substitution was checked by proton NMR spectra and elemental analysis for carbon. The degree of substitution was more than 90 % for o-ClPBDG, m-ClPBDG, and p-NPBDG, and 66 % for p-MePBDG. p-ClPBDG and p-ClPBLG were synthesized by the method of Ledger, et al.[14,15] p-ClPBDG + p-ClPBLG was prepared by dissolving equi-moles of p-ClPBDG and p-ClPBLG in chloroform. Films for dielectric measurements of o-Cl PBDG, m-ClPBDG, p-ClPBDG, and p-MePBDG were prepared by casting concentrated chlorofom solution on a glass plate at room temperature. A film of p-NPBDG was made from concentrated m-cresol solution at 50°C. Silver electrodes were vacuum deposited on both surfaces of film to assure complete electric contact. Each film was set in the measuring cell and evacuated at a temperature of 150°C until the dielectric constant remained unchanged.

The dielectric constant and loss factor were measured by the same apparatus and procedure as used in the preceding chapter. Measurements were made over a frequency range from 30Hz to 300kHz and at temperatures ranging from -150 to 120°C.

Samples used for broad-line NMR measurements were in a form of powder freeze-dried from dioxane solutions. Before measurement, each sample was evacuated at a temperature of

100°C for 48 hrs to eliminate residual solvent.

A JEOL JNS-B spectrometer was employed for obtaining derivatives of broad-line proton NMR absorption curves. The temperature was varied from liquid nitrogen temperature to about 100°C.

III-2. RESULTS

A. o-ClPBDG, m-ClPBDG, and p-ClPBDG

Figure 3.1 shows the temperature dependence of the dielectric constant ε' and the loss factor ε'' measured at a frequency of 1kHz for o-ClPBDG, m-ClPBDG, and p-ClPBDG. The data for PBLG are also shown for comparison. For each sample, a remarkable dielectric dispersion was observed above room temperature. The dispersion observed for PBLG has been interpreted in terms of the onset of side-chain motions.[16] NMR,[17-19] dynamic mechanical,[19,20] and dielectric measurements[21,19] for PBLG and other poly(glutamate)s have provided a great deal of evidence to support this interpretation. Thus, it is reasonable to consider that dielectric dispersions observed above room temperature for the samples of monochloro-PBDG are attributed to the same origin as PBLG. The dielectric constant was of the order m-ClPBDG > o-ClPBDG > p-ClPBDG ≃ PBLG in the temperature range of -50—0°C.

Figure 3.2 shows the results of NMR measurements for o-ClPBDG, m-ClPBDG, and p-ClPBDG; the second moment of the absorption line is plotted against temperature. Experimental points were omitted for the sake of clarity. Data for PBLG are also shown in the figure as a dotted line. It was found that the second moments for all samples studied decrease with increasing temperature in two steps. In the temperature range from -140 to -20°C, the second moments

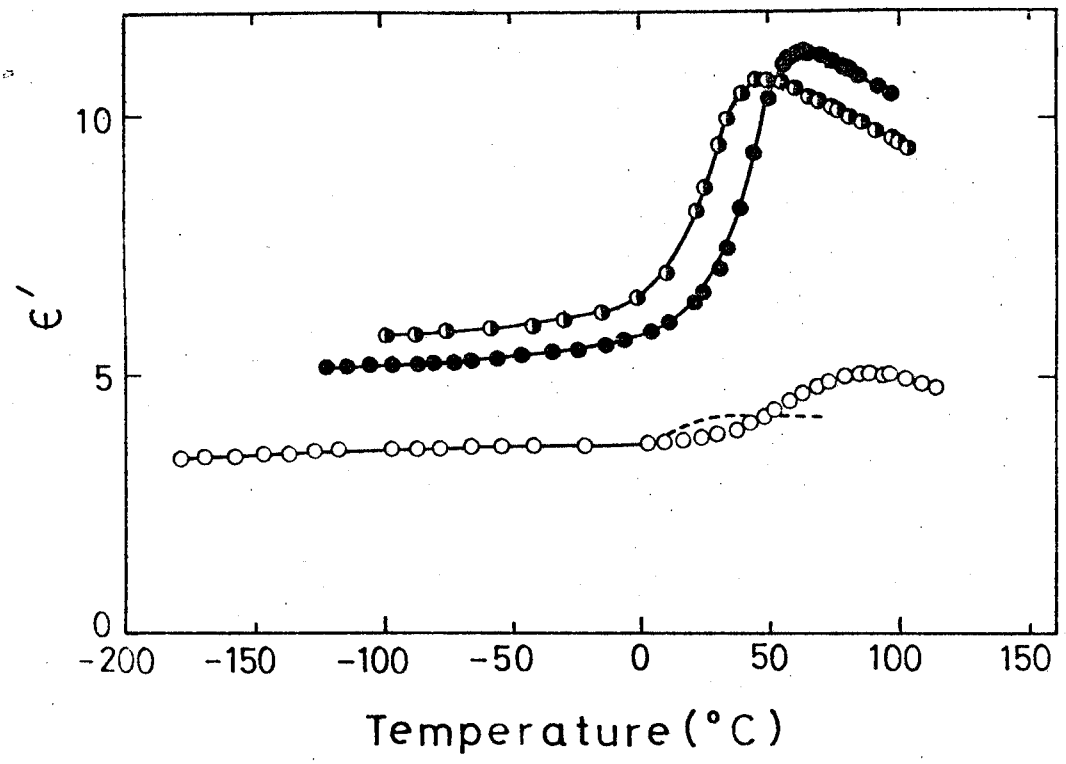

Figure 3.1 (a). Temperature dependence of the dielectric constant ε' of o-ClPBDG(●), m-Cl PBDG(◑), p-ClPBDG(○), and PBLG(----)measured at 1kHz.

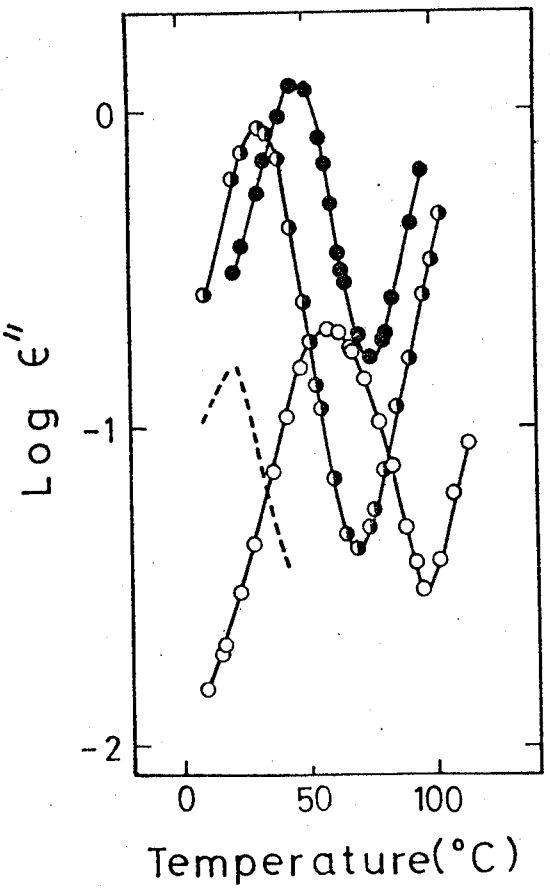

Figure 3.1 (b). Temperature dependence of the loss factor ε'' of o-ClPBDG(●), m-ClPBDG(◑), p-ClPBDG(○), and PBLG(-----) measured at 1kHz.

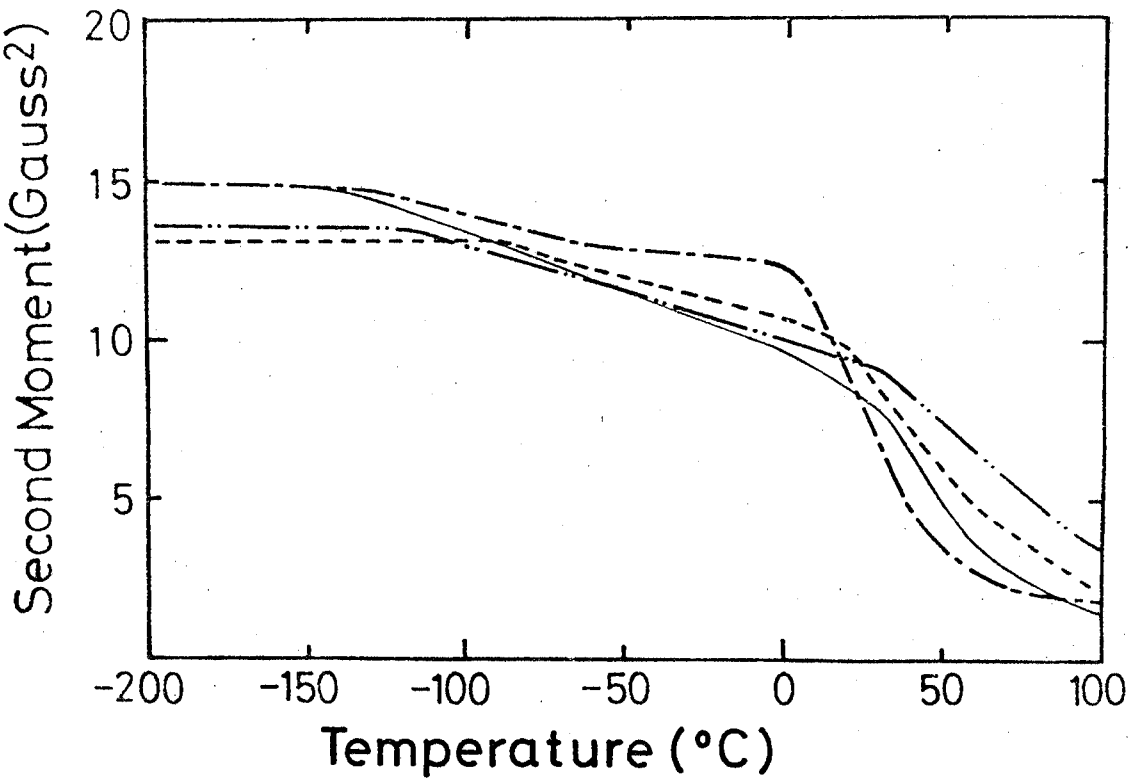

Figure 3.2. The second moment of monochloro-PBDGs as a function of temperature: ------, o-ClPBDG; ——————, m-ClPBDG; ——·——, p-ClPBDG; ———————, PBLG.

decrease gradually with increasing temperature. The decrease in second moment in this temperature range may be attributed to the rotation of the phenyl ring as is the case of PBLG.[17-19] Above room temperature, all samples show an abrupt decrease in second moment which is related to the appearance of the dielectric side-chain dispersion in the same temperature range.

Figure 3.3 shows the frequency dependence of ε' and ε'' for o-ClPBDG at various temperatures from 21.5 to 70.2°C. It is apparent that o-ClPBDG shows a dielectric dispersion in this temperature range. All other samples show similar frequency dependence as o-ClPBDG.

In Figure 3.4, the temperature dependences of the relaxation strength $\Delta\varepsilon = \varepsilon_0 - \varepsilon_\infty$ are shown for o-ClPBDG, m-ClPBDG, p-ClPBDG, and PBLG. The relaxation strength was determined by the Cole-Cole plot. It was found that the relaxation strength $\Delta\varepsilon$ is in the order o-ClPBDG > m-ClPBDG > p-ClPBDG $\simeq$ PBLG, and that a maximum appears in the $\Delta\varepsilon$--temperature curve.

After normalizing $\varepsilon' - \varepsilon_\infty$— and ε''— frequency curves by $\Delta\varepsilon$ all data were able to be superposed on a master curve at a certain temperature by performing suitable horizontal translations along the logarithmic frequency axis. The master curves of the loss factor for o-ClPBDG, m-ClPBDG, p-ClPBDG, and PBLG are compared in Figure 3.5, where the normalized loss factor is represented in units of its maximum value and the reduced frequency in units of the value at which the maximum occurs. It is apparent that the substi-

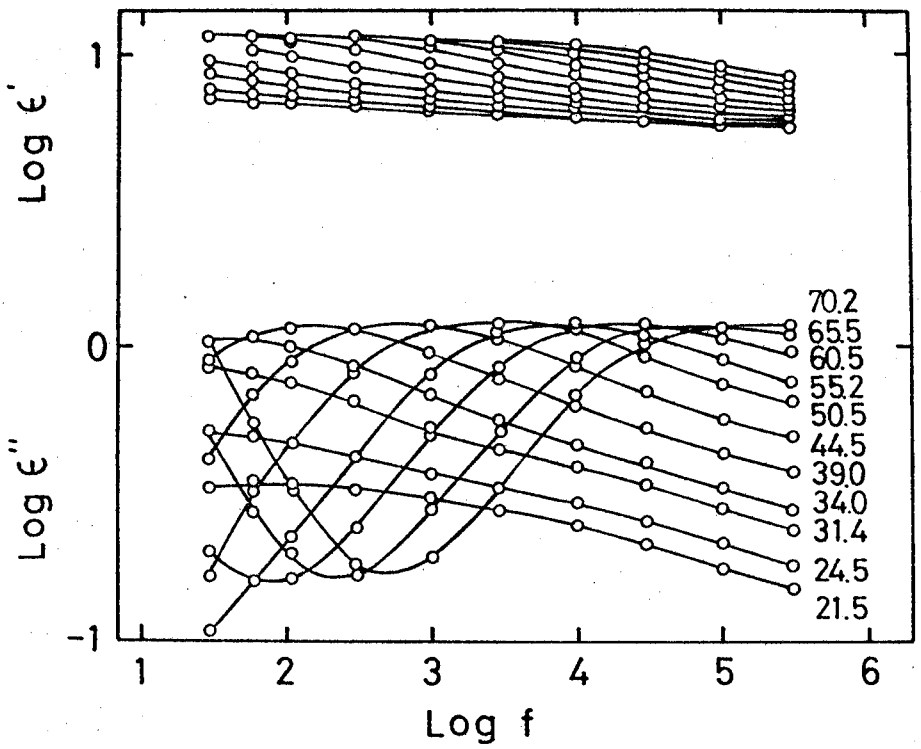

Figure 3.3. The dielectric constant ε' and the loss factor ε" for o-ClPBDG as a function of the logarithm of frequency f at indicated temperatures.

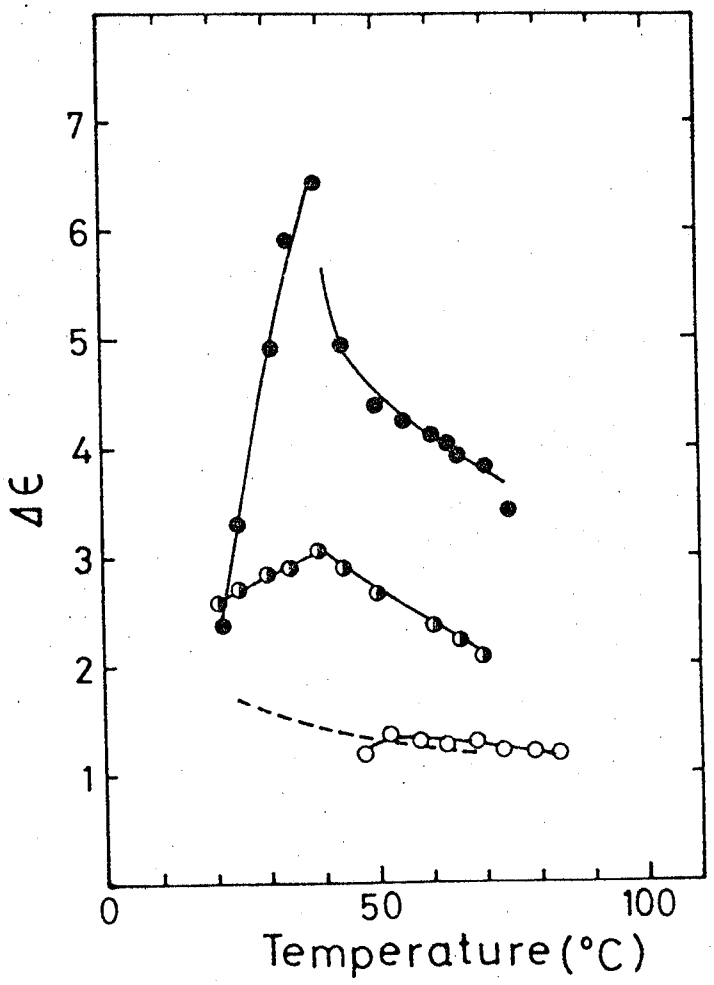

Figure 3.4. Temperature dependence of the relaxation strength Δε obtained from the Cole-Cole plot of monochloro-PBDGs: o-ClPBDG(●), m-ClPBDG(◑), p-ClPBDG(○), and PBLG(-----).

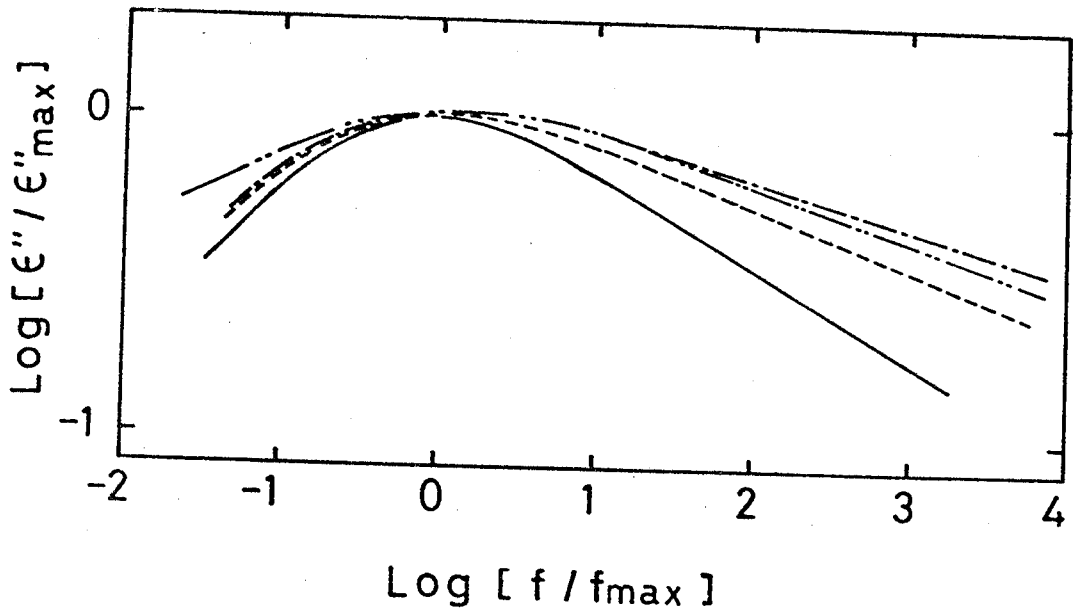

Figure 3.5. Composite master curves of the loss factor $\varepsilon'' / \varepsilon''_{max}$ for monochloro-PBDG: -------, o-ClPBDG; ———, m-ClPBDG; ——, p-ClPBDG; ———, PBLG.

tution of chlorine atom at the phenyl ring of PBDG causes the dispersion much more broader.

B. p-NPBDG, p-ClPBDG, and p-MePBDG

Figure 3.6 shows the temperature dependence of the dielectric constant ε' and the loss factor ε'' measured at 1kHz for p-NPBDG, p-ClPBDG, p-MePBDG, and PBLG. Each sample clearly shows a dielectric dispersion which is attributed to the side-chain motion by the same reason as described previously for monochloro-PBDG. Considerably higher dispersion temperature of p-NPBDG implies that there exist strong constraints on side-chain motions.

Master curves of the loss factor for p-NPBDG, p-ClPBDG, p-MePBDG, and PBLG which were obtained by the same procedure as described in the preceding section are compared in Figure 3.7. It is apparent that the master curve of the loss factor is much broader for p-substituted PBDGs than for PBLG. Among monosubstituted PBDGs studied here, p-NPBDG and p-MePBDG show much broader dispersion curves.

C. p-ClPBDG and p-ClPBDG + p-ClPBLG

Figure 3.8 shows the temperature dependence of the dielectric constant ε' and the loss factor ε'' measured at 1kHz for p-ClPBDG and p-ClPBDG + p-ClPBLG. In each sample, two dielectric dispersions are observed, the one located at

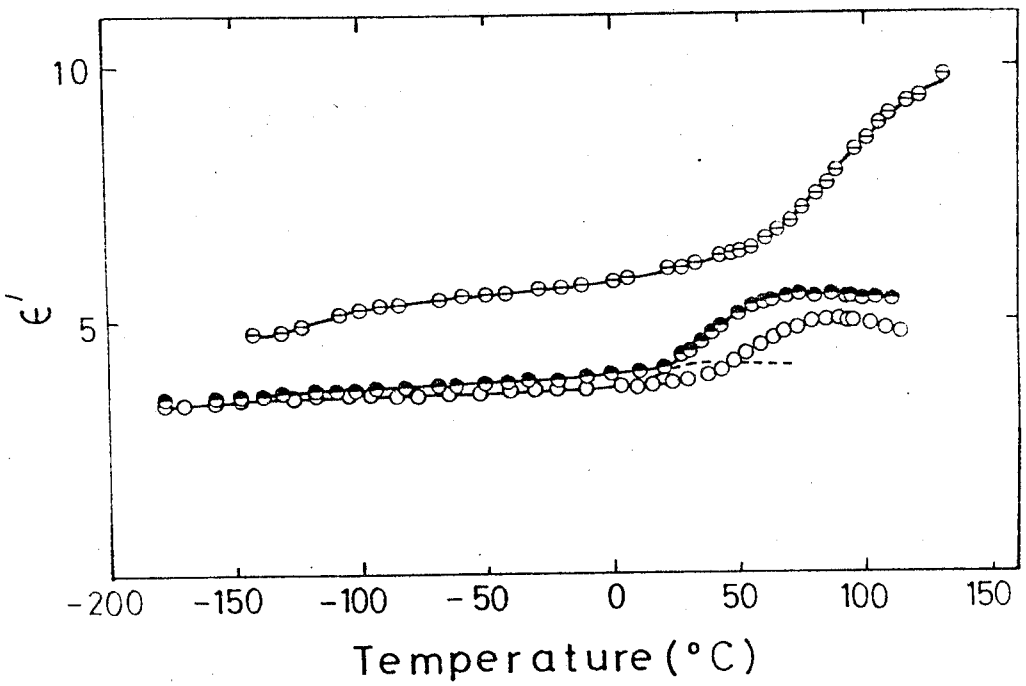

Figure 3.6 (a). Temperature dependence of the dielectric constant ε'of p-NPBDG(⊖), p-MePBDG(◓), p-ClPBDG(○), and PBLG(---) measured at 1kHz.

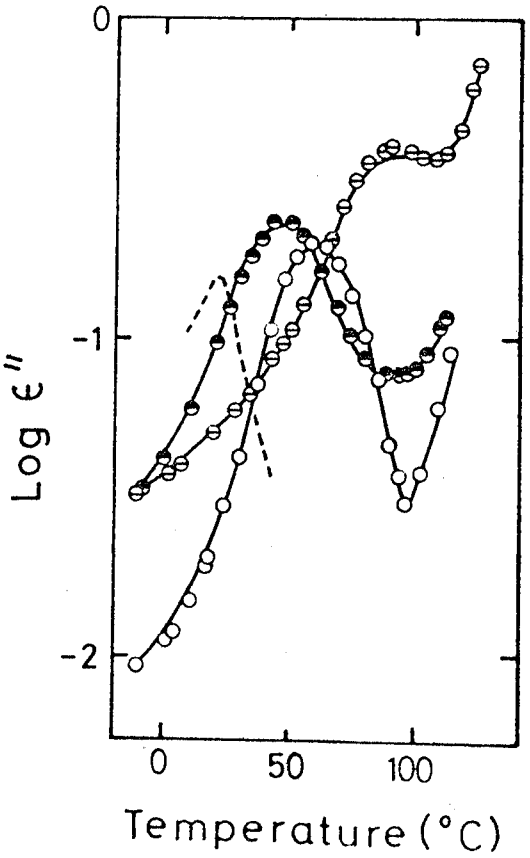

Figure 3.6 (b). Temperature dependence of the loss factor ε" of p-NPBDG(⊖), p-MePBDG (◓), p-ClPBDG(○), and PBLG(-----) measured at 1kHz.

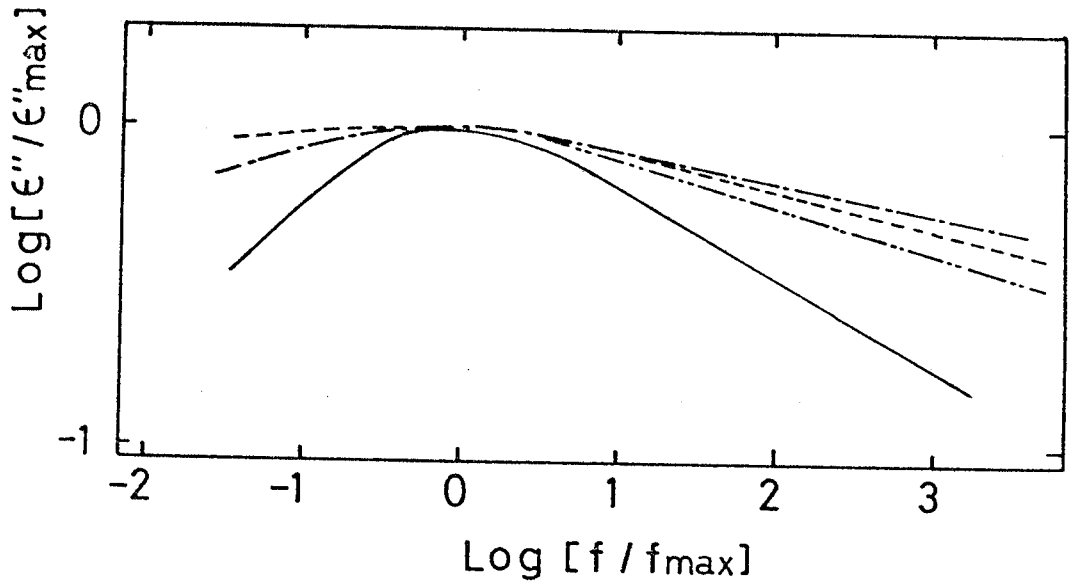

Figure 3.7. Composite master curves of the loss factor $\varepsilon'' / \varepsilon''_{max}$ for p-monosubstituted PBDG: -------, p-NPBDG; ———, p-MePBDG; — — —, p-ClPBDG; ————, PBLG.

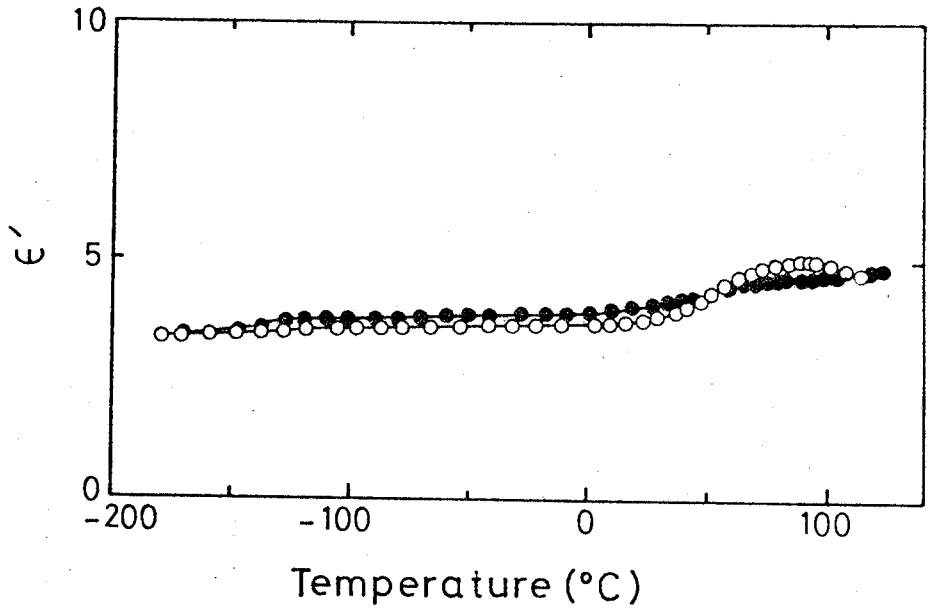

Figure 3.8 (a). Temperature dependence of the dielectric constant ε' of p-ClPBDG(○) and p-Cl PBDG + p-ClPBLG(●) measured at 1kHz.

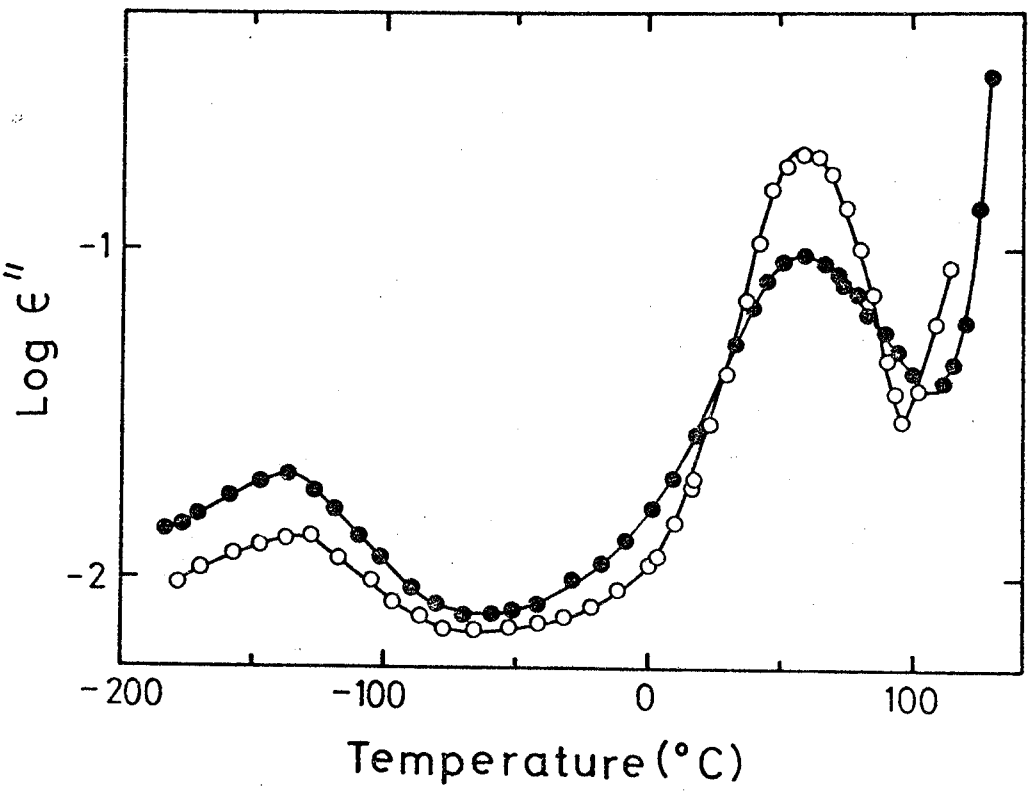

Figure 3.8. Temperature dependence of the loss factor ε" of p-ClPBDG(○) and p-ClPBDG + p-ClPBLG(●) measured at 1kHz.

about 60°C(dispersion I) and the other located far below room temperature(dispersion II). As already mentioned before, dispersion I is assigned to the onset of the large scale motion of the side chain, while dispersion II is considered due to the vibrational local motion of the side chain.[19,22,23]

As for the dispersion temperature of dispersion I, the two samples show the same temperature of 60°C, on the other hand, for dispersion II, p-ClPBDG + p-ClPBLG shows a dispersion temperature lower than p-ClPBDG by some 10°C. Such lowering of the dispersion temperature of dispersion II by racemic mixing has been also reported for PBLG + PBDG.[24]

In Figure 3.9 is shown the temperature dependence of the relaxation strength $\Delta\varepsilon$ obtained by the Cole-Cole plot. $\Delta\varepsilon$ for the racemic mixture increases monotonously with increasing temperature, while for p-ClPBDG, $\Delta\varepsilon$ vs. temperature curve has a maximum at a certain temperature. The value of $\Delta\varepsilon$ of the racemic mixture is smaller than that of p-Cl PBDG.

The time—temperature superposition principle was also applicable for dispersion I of p-ClPBDG + p-ClPBLG. The results of p-ClPBDG and p-ClPBDG + p-ClPBLG are shown in Figure 3.10, of which the ordinate and abscissa are the same as in Figure 3.5. The master curve for p-ClPBDG + p-ClPBLG is found to be broader than that for p-ClPBDG.

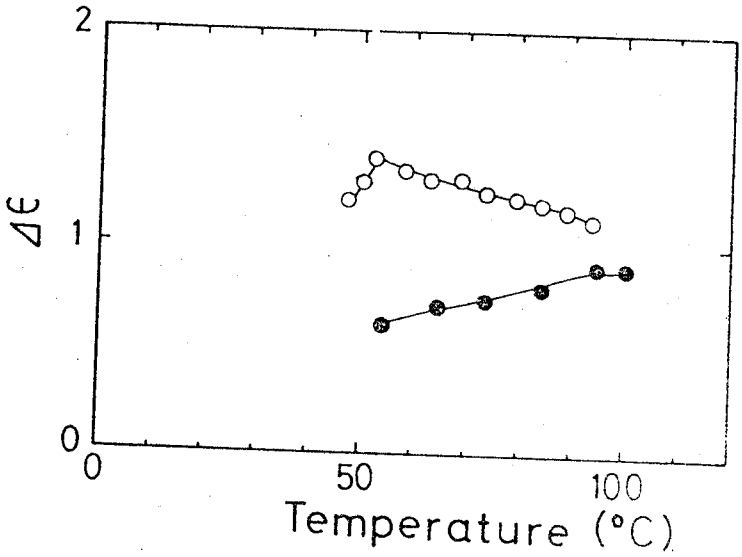

Figure 3.9. Temperature dependence of the relaxation strength Δε obtained from the Cole-Cole plot of p-ClPBDG(○), and p-ClPBDG + p-ClPBLG(●).

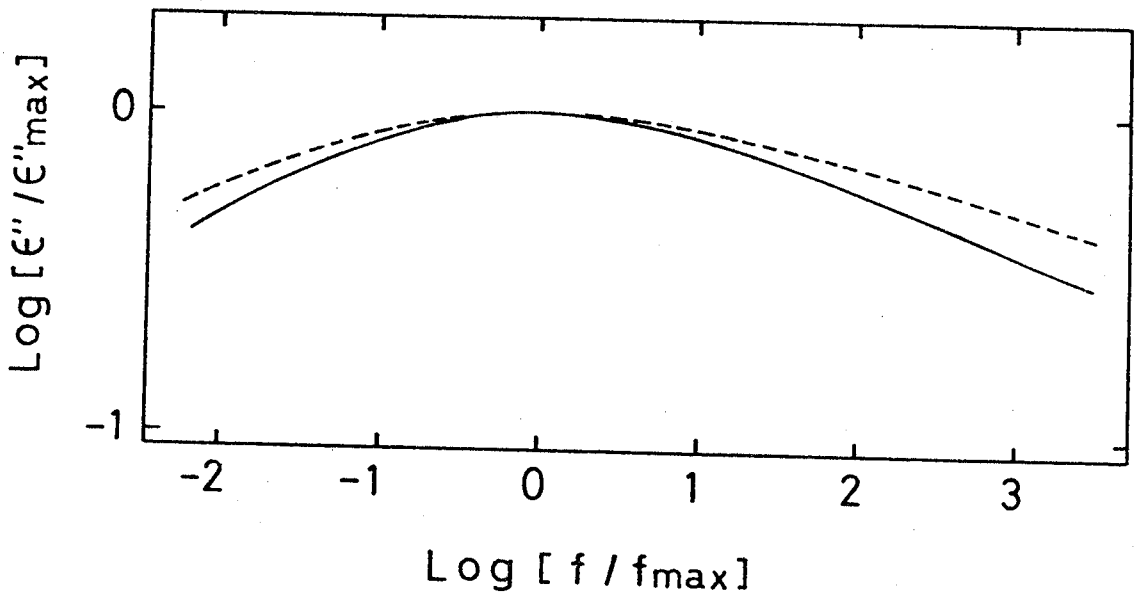

Figure 3.10. Composite master curves of the loss factor $\varepsilon'' / \varepsilon''_{max}$ of p-ClPBDG(————) and p-ClPBDG + p-ClPBDG(-------).

III-3. DISCUSSION

The appearance of a maximum in the $\Delta\varepsilon$-temperature curve for all samples except for p-ClPBDG + p-ClPBLG suggests that the observed dispersion for each sample has a property reminiscent of the glass transition of the synthetic amorphous polymer. This suggestion was also intimated by the temperature dependence of the shift factor b_T obtained by the superposition procedure. It was found that b_T follows the WLF equation.[20,25] Table III-1 shows the dispersion temperature T_{max} which is defined as the temperature of the loss maximum at a frequency of 1kHz for monosubstituted PBDG along with PBLG for comparison. The dispersion temperatures of all monosubstituted PBDGs are higher than that of PBLG. This implies that the introduction of the substituent into the phenyl ring gives rise to restrictions on side-chain motions. The broader master curve of monosubstituted PBDG in comparison with that of PBLG also suggests the existence of such a restriction.

The influence of the introduction of the substituent into the phenyl ring on molecular motions has been reported for polystyrene.[26,27] Barb pointed out various ways by which the softening point of polystyrene can be elevated. (1) Substitution for specifically causing intramolecular steric hinderance between the substituent and vicinal main-chain segments; large rigid o-substituents produce such an effect. (2) Substitution to increase steric hinderance between the phenyl ring and the neighboring polymers.

Table III-1 Dielectric dispersion temperature

Sample	T_{max} (°C)
o-ClPBDG	47
m-ClPBDG	32
p-ClPBDG	60
p-NPBDG	90
p-MePBDG	47
p-ClPBDG + p-ClPBLG	60
PBLG	25

T_{max} , dielectric dispersion temperature defined as the temperature of the loss maximum at a frequency of 1kHz.

Large rigid groups at an " exposed " position, particularly at the p-position, have this effect. (3) Substitution by dipolar group to produce long-range dipole—dipole interaction, as in the case of poly(p-chlorostyrene).

This explanation can be also applied to the present case. In our case, T_{max} may be taken as a measure of the restriction acting on side-chain motions. It is in the following order: for monochloro-PBDGs, p-ClPBDG(60°C) > o-ClPBDG(47°C) > m-ClPBDG(32°C) > PBLG(25°C), and for p-monosubstituted PBDGs, p-NPBDG(90°C) > p-ClPBDG(60°C) > p-Me PBDG(47°C).

The highest T_{max} for p-ClPBDG in the former series indicates that (2) is a dominant effect, while for polystyrene (1) is most effective. The difference in structure between polystyrene and the side chain of PBDG may be responsible for the lesser effectiveness of (1) in the present case. For polystyrene, the phenyl ring is connected to biforked polymer segments at its root, but for the side chain of PBDG, it is connected to only one side-chain segment.

The estimation of allowed conformations of the side chain of monochloro-PBDGs was made by the Monte Carlo calculation using an electronic computer.[28] The results showed that for p-ClPBDG, the chlorine atom is likely to be located in outermost parts of the side-chain region surrounding the α-helical backbone, while for o-ClPBDG the chlorine atom is located more or less in the inner parts

of the side-chain region. Thus, the dipole—dipole interaction between " exposed " dipoles of neighboring molecules for p-ClPBDG may be more effective than the steric hindrance between the substituent and the other part of the side chain.

The enormous relaxation strength of o-ClPBDG suggests that the side chain of o-ClPBDG may take a conformation with a large resultant dipole moment by the short range correlation of the C=O dipole and the C—Cl dipole or by the side chain—backbone chain interaction. Scheraga et al. have calculated the minimum energy conformation of the side chain of poly[β-(o-chlorobenzyl) aspartate], which has a shorter side chain than o-ClPBDG by one methylene group but otherwise is very similar.[29] A conformation proposed by these authors gives a value of 2.7 Debye for dipole moment of the side chain, which is obviously larger than a value of 1.4 Debye calculated without considering the correlation of C=O and C—Cl dipoles.

The highest T_{max} of p-NPBDG indicates the existence of strong contributions from the long range dipole interaction and the sizable volume of the nitro group to the restriction on side-chain motions. The effect may be enhanced by the substitution at the " exposed " position. In Figure 3.11, the dispersion temperature T_{max} is plotted against the mean square of the dipole moment of p-substituted phenyl rings in order to examine the correlation between the polarity and the restriction on side-chain motions. The value of the dipole moment was taken from a literature.[30] It is found that there is a definite

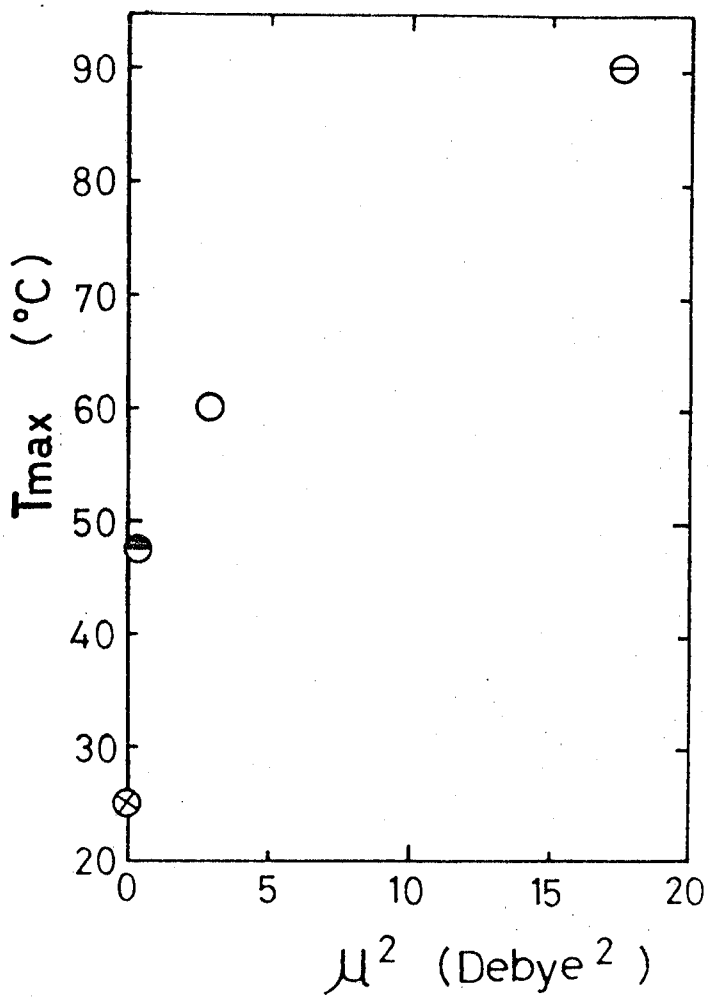

Figure 3.11. The dispersion temperature T_{max} plotted against the square of the dipole moment of substituted benzyl groups; that of p-NPBDG(⊖), of p-ClPBDG(○), of p-MePBDG(◓) and of PBLG (⊗).

correlation between values of T_{max} and the mean square of the dipole moment $< \mu^2 >$. These results suggest that the contribution of dipole—dipole interaction to restrict side-chain motions is appreciable.

As mentioned in the results section, the liberation of the phenyl ring rotation around the benzyl methylene carbon and phenyl ring carbon bond (C_ζ—C_ϕ) occurs at lower temperatures. Since the decrement of the second moment in the temperature range between -140 and 0°C is almost the same for each polymer, the phenyl ring in each sample is likely to rotate in a similar way. The effect of the liberation of rotation of the phenyl ring upon the dielectric constant depends on the position of the substitution of polar group. In the case of p-ClPBDG, since the direction of the C—Cl dipole agrees with the rotation axis, the phenyl ring rotation shoud be ineffective in changing the direction of the dipole moment, and the dielectric constant should be equal to that of PBLG in a temperature range where only rotation of C_ζ—C_ϕ occurs. But, in the case of o-ClPBDG and m-ClPBDG, the contribution from the C—Cl dipole to the dielectric constant is significant. The somewhat smaller value of o-ClPBDG in comparison with that of m-isomer seems to be caused by the steric hindrance between the O—C=O and C—Cl groups.

Racemic mixture of PBDG and PBLG(PBDG + PBLG) has been reported to show an extra meridional X-ray reflection of 10.6 Å attributable to the phenyl ring stacks in the side chains.[7-12] The previous dielectric measurements showed

that the first-order phase transition due to the break down of the stacks occurs at about 90°C for PBDG + PBLG. For a racemic mixture of p-ClPBDG and p-ClPBLG, no reflections reminiscent of the stack were observed.[4] Furthermore, any evidence for the first-order transition could not be observed in this study. The large dipole moment and large volume of chlorine atom seem to prevent stacking for p-Cl PBDG + p-ClPBLG. The dispersion temperatures of the dispersion I for p-ClPBDG and for p-ClPBDG + p-ClPBLG are almost the same. The relaxation strength for p-ClPBDG + p-ClPBLG is, however, smaller than that of p-ClPBDG and monotonously increases with temperature. It is likely that the dipole—dipole interaction between " exposed " dipoles is more effective for p-ClPBDG + p-ClPBLG than p-ClPBDG.

REFERENCES

1. Y. Konishi and M. Hatano, J. Polym. Sci. Polym. Lett. Ed., 14, 303 (1976).
2. Y. Konishi and M. Hatano, J. Polym. Sci. Polym. Lett. Ed., 14, 351 (1976).
3. Y. Konishi and M. Hatano, J. Polym. Sci. Polym. Lett. Ed., 14, 2329 (1976).
4. M. Osanai, A. Tsutsumi, K. Hikichi, M. Kaneko, Y. Konishi, and M. Hatano, Rep. Prog. Polym. Phys. Jpn., 19, 517 (1976).
5. M. Osanai, A. Tsutsumi, K. Hikichi, Y. Konishi, and M. Hatano, Rep. Prog. Polym. Phys. Jpn., 20, 589 (1977).
6. M. Chien, E. T. Samulski, and C. G. Wade, Macromolecules, 6, 683 (1973).
7. M. Tsuboi, A. Wada, and N. Nagashima, J. Mol. Biol., 3, 705 (1961).
8. A. Elliott, R. D. B. Fraser, and T. P. MacRae, J. Mol. Biol., 11, 821 (1965).
9. Y. Mitsui, Y. Iitaka, and M. Tsuboi, J. Mol. Biol., 24, 15 (1967).
10. J. M. Squire and A. Elliott, J. Mol. Biol., 65, 291 (1972).
11. T. Takahashi, A. Tsutsumi, K. Hikichi, and M. Kaneko, Macromolecules, 7, 806 (1974).
12. N. Matsushima, K. Hikichi, A. Tsutsumi, and M. Kaneko, Polym. J., 7, 382 (1975).

13. E. M. Bradbury, B. G. Carpenter, and H. Goldman, Biopolymers, 6, 837 (1968).

14. R. Ledger and F. H. C. Stewart, Aust. J. Chem., 18, 1477 (1965).

15. R. Ledger and F. H. C. Stewart, Aust. J. Chem., 19, 1729 (1966).

16. K. Hikichi, K. Saito, M. Kaneko, and J. Furuichi, J. Phys. Soc. Jpn., 19, 557 (1964).

17. K. Hikichi, J. Phys. Soc. Jpn., 19, 2169 (1964).

18. A. Tsutsumi, Jpn. J. Appl. Phys., 9, 2225 (1970).

19. A. Tsutsumi, K. Hikichi, T. Takahashi, Y. Yamashita, N. Matsushima, M. Kanke, and M. Kaneko, J. Macromol. Sci.-Phys., B8, 413 (1973).

20. Y. Yamashita, A. Tsutsumi, K. Hikichi, and M. Kaneko, Polym. J., 8, 114 (1975).

21. A. Tsutsumi, K. Hikichi, M. Mitsumaki, and M. Kaneko, J. Phys. Soc. Jpn., 22, 1120 (1967).

22. K. Yamafuji, J. Phys. Soc. Jpn., 15, 2295 (1960).

23. R. Hayakawa and Y. Wada, J. Polym. Sci. Polym. Phys. Ed., 12, 2119 (1974).

24. K. Shimizu, O. Yano, and Y. Wada, Rep. Prog. Polym. Phys. Jpn., 18, 547 (1975).

25. M. L. Williams, R. F. Landel, and J. D. Ferry, J. Am. Chem. Soc., 77, 3701 (1955).

26. W. G. Barb, J. Polym. Sci., 37, 515 (1959).

27. R. D. McCammon and R. G. Saba, J. Polym. Sci., A-2, 7, 1721 (1969).

28. K. Hikichi, unpublished results.

29. J. F. Yan, F. A. Momang, and H. A. Scheraga, J. Am. Chem. Soc., 92, 1109 (1970).

30. L. Pauling, " Nature of the Chemical Bond," Cornell University Press, Ithaca, New York, N. Y., 1960.

CHAPTER IV

DIELECTRIC PROPERTIES OF POLY(ε-N-BENZYLOXYCARBONYL-L-LYSINE) IN THE SOLID STATE AND HYDROGEN BONDS OF THE SIDE CHAIN

In our previous papers,[1-3] it was reported that the behavior of the side-chain dispersion of poly(ε-N-benzyloxycarbonyl-L-lysine)(PCLL) is well described by the WLF-equation, as is true in the case of PBLG and PMLG.[4,5]

In Chapter II, the relationship between the length of the side chain of poly(alkyl glutamate)s and the side-chain mobility was examined. The increase in the side-chain length was found to enhance the side-chain mobility. Thus, it may be expected that the dispersion temperature of PCLL might be far below those of PBLG and PMLG, because the side chain of PCLL is much longer than those of PBLG and PMLG. Contrary to this expectation, the dispersion temperature of PCLL is higher than those of PMLG and PBLG.[1-4,6]

In this chapter, in order to explain this unexpected fact, dielectric solid-state properties of PCLL, a mixture of PCLL and PBDG(PCLL + PBDG), and a copolymer of ε-N-benzyloxycarbonyl-L-lysine and γ-benzyl D-glutamate(PCLBG) were examined.

Hatano and Yoneyama reported that for poly(α-amino acid)s having the urethane group in the side chain, such as for PCLL, poly(δ-N-benzyloxycarbonyl-L-ornithine), and poly(γ-N-benzyloxycarbonyl-L-α,γ-diaminobutyric acid), the urethane group in the side chain is hydrogen-bonded to those

in the neighboring side chain in chloroform-dichloroacetic acid solution. Thus, it will be reasonable to assume that the hydrogen bonding occurs in the solid state as well. The purpose of this study is to present an evidence of the hydrogen bonding in the solid state and to correlate the dielectric properties with the hydrogen bonding.

IV-1. EXPERIMENTAL

PCLL and PCLBG were prepared by polymerizing their respective NCA's in dioxane with a trace of triethylamine as an initiator. To obtain PCLBG, equi-moles of CLL-NCA and BLG-NCA were polymerized. The ratio of BLG- and CLL-residues in the copolymer was determined by the amino acid analysis and was found to be BLG : CLL = 2 : 1. PCLL + PBDG was prepared by dissolving equi-moles of PCLL and PBDG in N,N-dimethylformamide(DMF). Films for measurements were cast from concentrated DMF solutions on a glass plate at 50°C. Films were painted with conductive silver paste in order to assure complete contact with the electrodes. Each film was set in the measuring cell and evacuated at a temperature of 120 - 150°C until the dielectric constant at the temperature became constant.

The apparatus and procedure for dielectric measurements are the same as in preceding chapters.

Measurements were made over the frequency range from 110Hz to 1MHz. The temperature was changed from -150 to 100°C.

Films for measurements of infrared absorption spectra were obtained by evaporation to dryness of viscous DMF solution. The orientation was produced by unidirectional shearing of the viscous solution. The best oriented film was chosen after examination under a polarizing microscope. Infrared absorption spectra were recorded on a Hitachi EPI-G3 spectrometer.

IV-2. RESULTS AND DISCUSSION

Figure 4.1 shows the temperature dependence of the dielectric constant ε' and the loss factor ε'' measured at 1kHz for PCLL, PCLL + PBDG, and PCLBG. Two dielectric dispersions were observed at about 50°C and -70°C for each sample.

According to previous NMR[6] and dynamic mechanical[1,2,7] measurements for PCLL, the dispersion observed near room temperature is considered to be caused by the micro-Brownian motion of the whole side chain, and the dispersion observed far below room temperature is due to the oscillational motion of the side chain on a small scale.[8,9] The dielectric dispersions observed for PCLL + PBDG and PCLBG are assigned to the same origins as PCLL. In this chapter, only the dispersion near room temperature will be discussed.

Figure 4.2 shows the frequency dependence of ε' and ε'' for PCLL at various temperatures from 40.0°C to 85.5°C. After normalization with the relaxation strength $\Delta\varepsilon$, all of these ε'- and ε''- frequency curves could be superposed on a set of frequency dependence curves at a certain temperature by performing suitable horizontal translations along the logarithmic frequency axis.

In Figure 4.3 is shown a set of master curves for PCLL obtained in this way. Figures 4.4 and 4.5 also show composite master curves for PCLL + PBDG and PCLBG, respectively. For all samples, the time temperature superposition principle was found to be well applicable. The shift factor b_T of

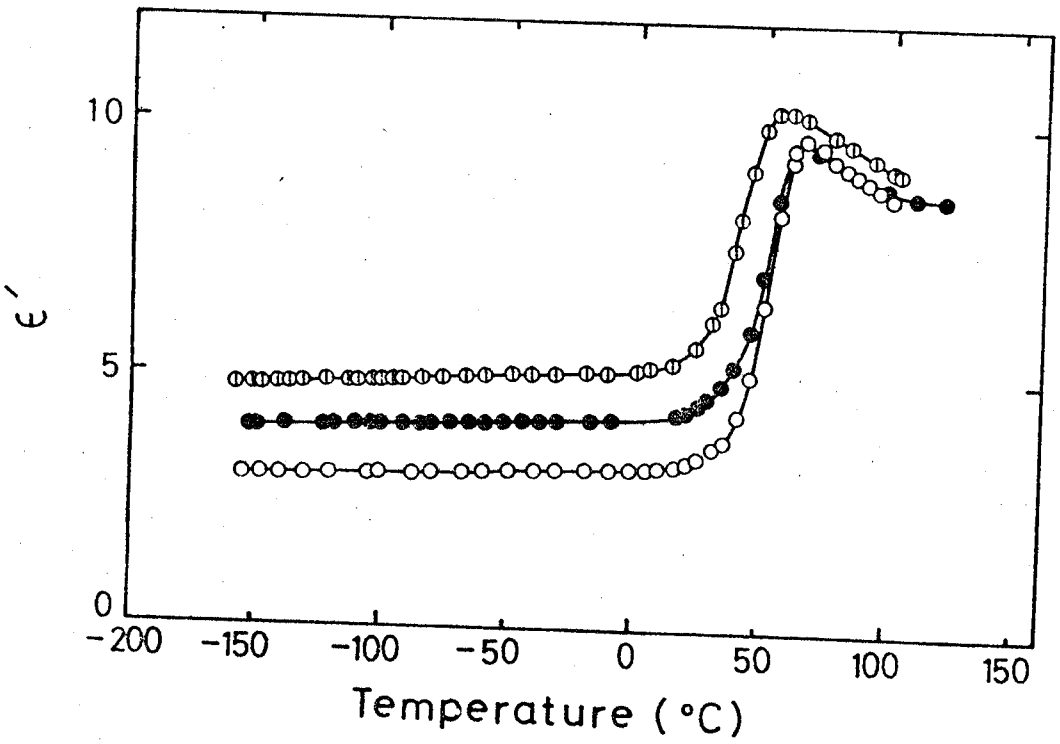

Figure 4.1 (a). Temperature dependence of the dielectric constant ε' for PCLL(○), PCLL + PBDG(●), and PCLBG(ⓘ) measured at 1kHz.

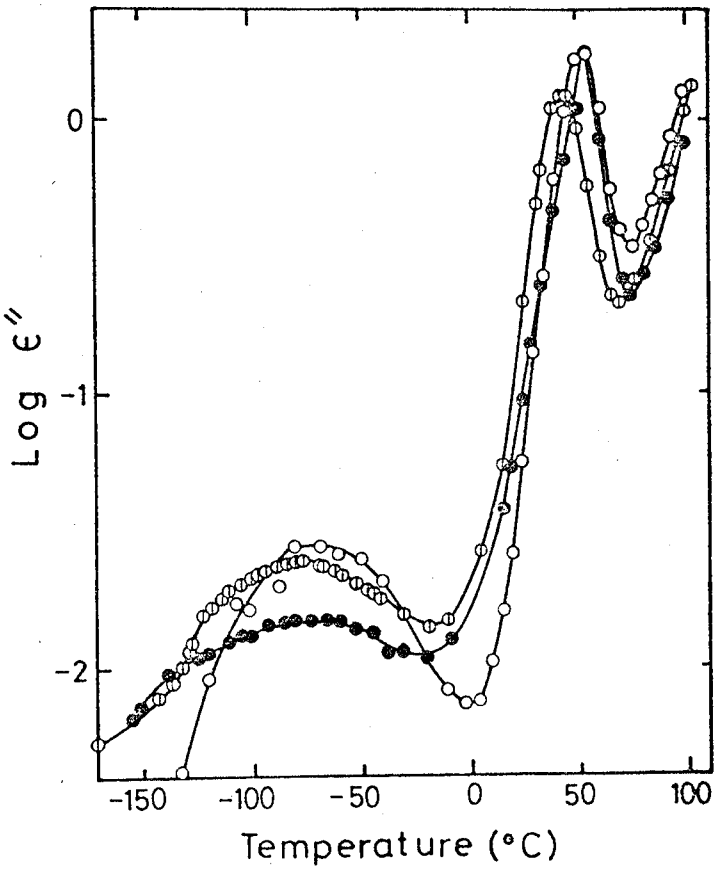

Figure 4.1 (b). Temperature dependence of the loss factor ε" for PCLL(◯), PCLL + PBDG(●), and PCLBG(◑) measured at 1kHz.

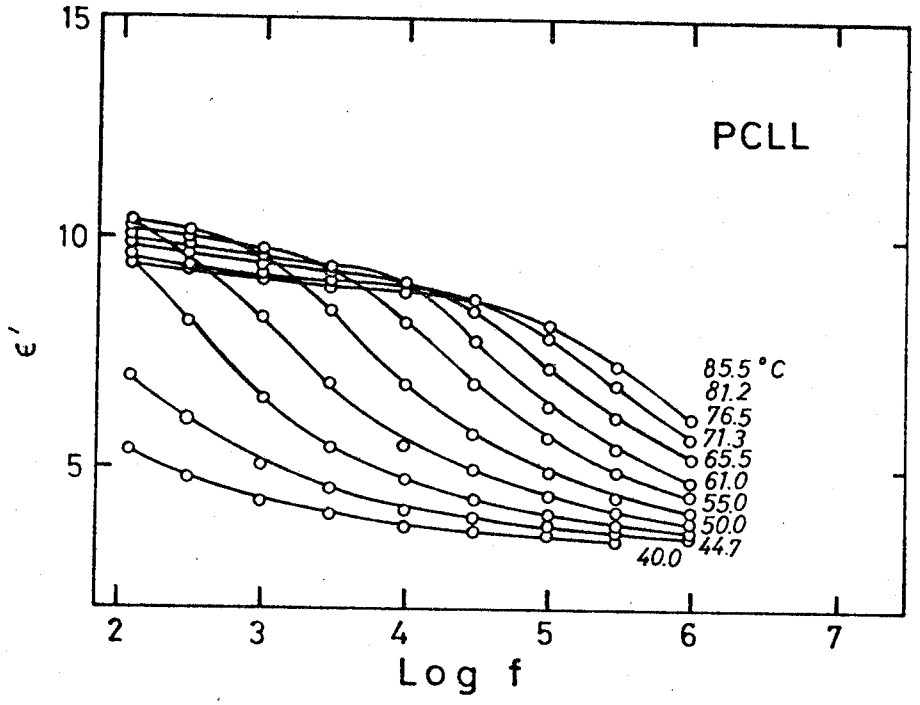

Figure 4.2 (a). Frequency dependence of the dielectric constant ε' for PCLL at indicated temperatures.

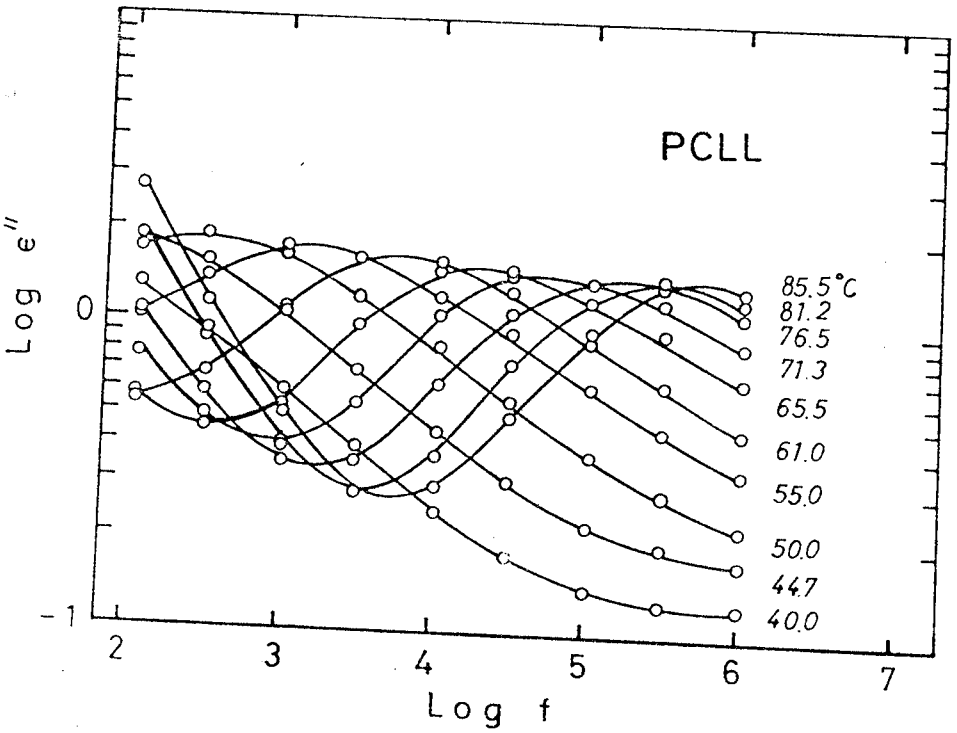

Figure 4.2 (b). Frequency dependence of the loss factor ε" for PCLL at indicated temperatures.

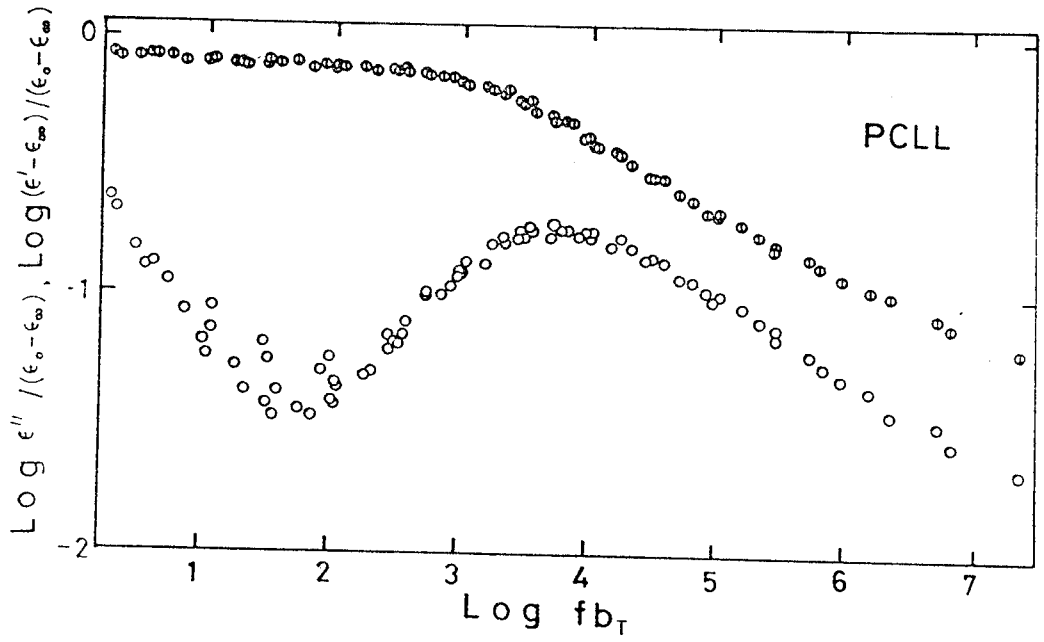

Figure 4.3. Composite dispersion curves of the normalized dielectric constant ($\varepsilon' - \varepsilon_\infty$)/ ($\varepsilon_0 - \varepsilon_\infty$) (⊕) and the loss factor $\varepsilon'' / (\varepsilon_0 - \varepsilon_\infty)$ (○) for PCLL reduced to 61.5°C. b_T is the shift factor.

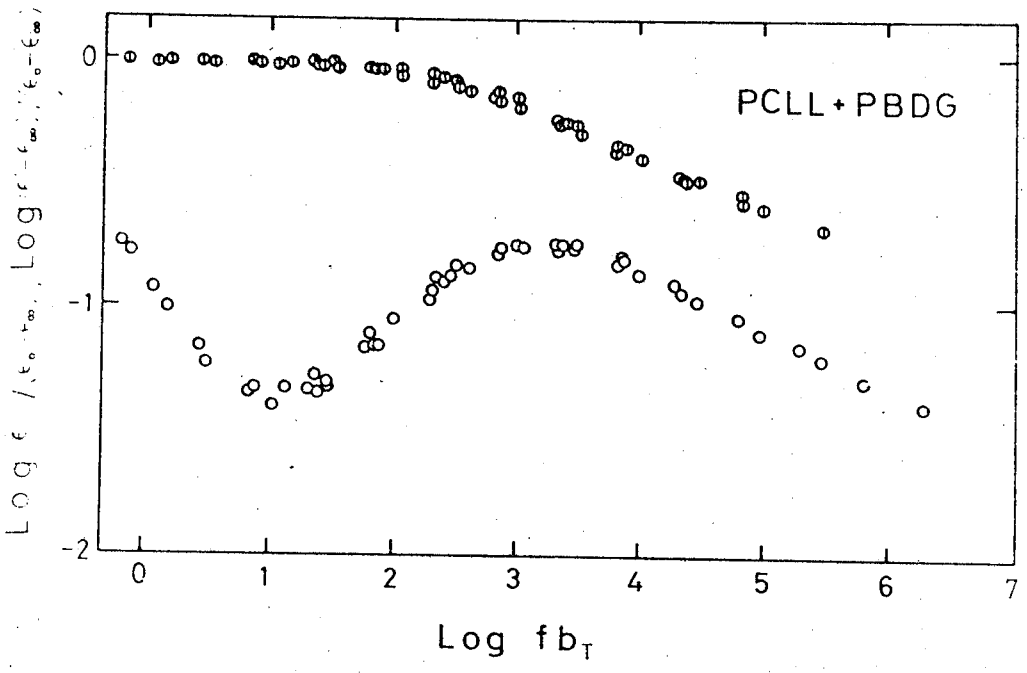

Figure 4.4. Composite dispersion curves of the normalized dielectric constant ($\varepsilon' - \varepsilon_\infty$)/ ($\varepsilon_0 - \varepsilon_\infty$) (◐) and the loss factor ε'' / ($\varepsilon_0 - \varepsilon_\infty$) (○) for PCLL + PBDG reduced to 60.5°C. b_T is the shift factor.

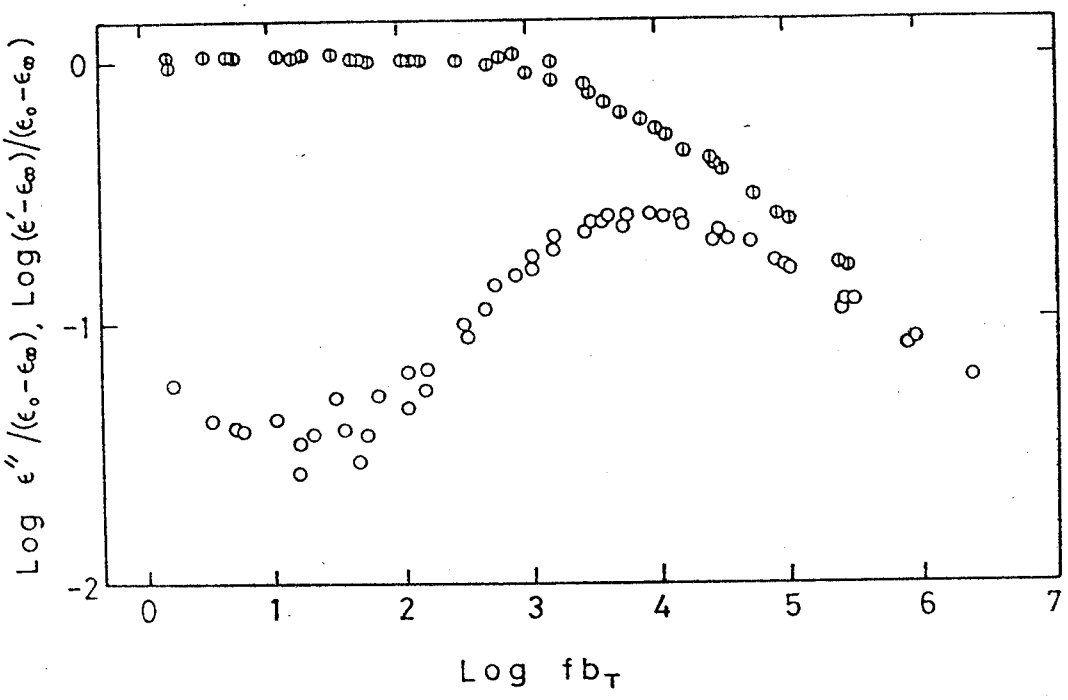

Figure 4.5. Composite dispersion curves of the normalized dielectric constant ($\varepsilon' - \varepsilon_\infty$)/($\varepsilon_0 - \varepsilon_\infty$) (⏀) and the loss factor ε'' /($\varepsilon_0 - \varepsilon_\infty$) (◯) for PCLBG reduced to 48.0°C. b_T is the shift factor.

PCLL + PBDG and PCLBG as well as PCLL were well described by the universal WLF-equation. Master curves of ε" for PCLL + PBDG and PCLBG show a single peak, and are as sharp as that of PCLL. This implies that side chains of the CLL-residue and the BLG- (or BDG-) residue of PCLL + PBDG and PCLBG undergo motions cooperatively.

Table IV-1 show the dispersion temperature T_{max}, the temperature of the loss maximum at a frequency of 1kHz, for PCLL, PCLL + PBDG, and PCLBG together with that of PBLG for comparison. Dispersion temperature of all samples measured here are obviously higher than that of PBLG. Thus, motion of side chains of these samples is remarkably restricted in the vicinity of room temperature compared with that of PBLG side chain. It is probable that there exists a strong interaction among the CLL-side chains.

Figures 4.6 (a), (b), and (c) show infrared absorption spectra of oriented films of PCLL, PCLL + PBDG, and PCLBG, respectively. In the NH-stretching absorption region of these polymers, two bands are observed: a free NH-band at 3400 cm^{-1} and a hydrogen-bonded NH-band at 3300 cm^{-1}. Two species are responsible for the free NH-stretching absorption band: one is the side-chain amide, the other is the amide group of the main chain when the α-helix is locally broken. The backbone chains of these polymers, however, are thought to be almost perfect α-helices. Since a number of evidences of the higher mobility of the side chain as compared with that of the main chain have been accumulated,[4,5] it may be reasonable to assign the free NH-stretching band

Table IV-1 Dielectric dispersion temperature

Sample	T_{max} (°C)
PCLL	55
PCLL + PBDG	55
PCLBG	43
PBLG	30 [a]

a, Ref 4.

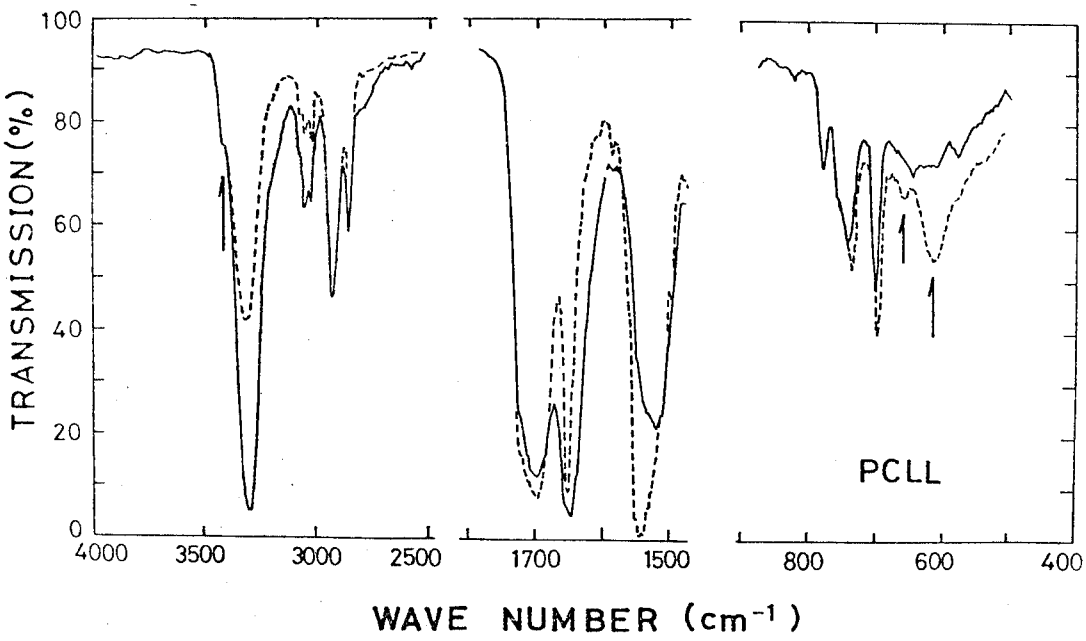

Figure 4.6 (a). Polarized infrared absorption spectrum of PCLL: ------, electric vector perpendicular to the orientation direction; ———, electric vector parallel to the orientation direction.

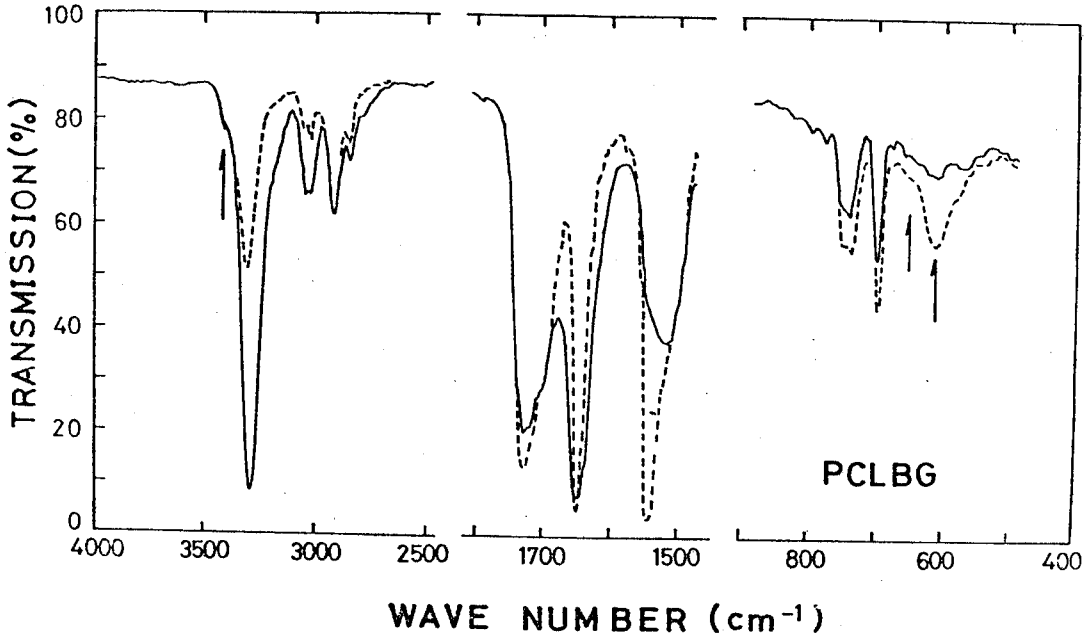

Figure 4.6 (b). Polarized infrared absorption spectrum of PCLL + PBDG: ------, electric vector perpendicular to the orientation direction; ———, electric vector parallel to the orientation direction.

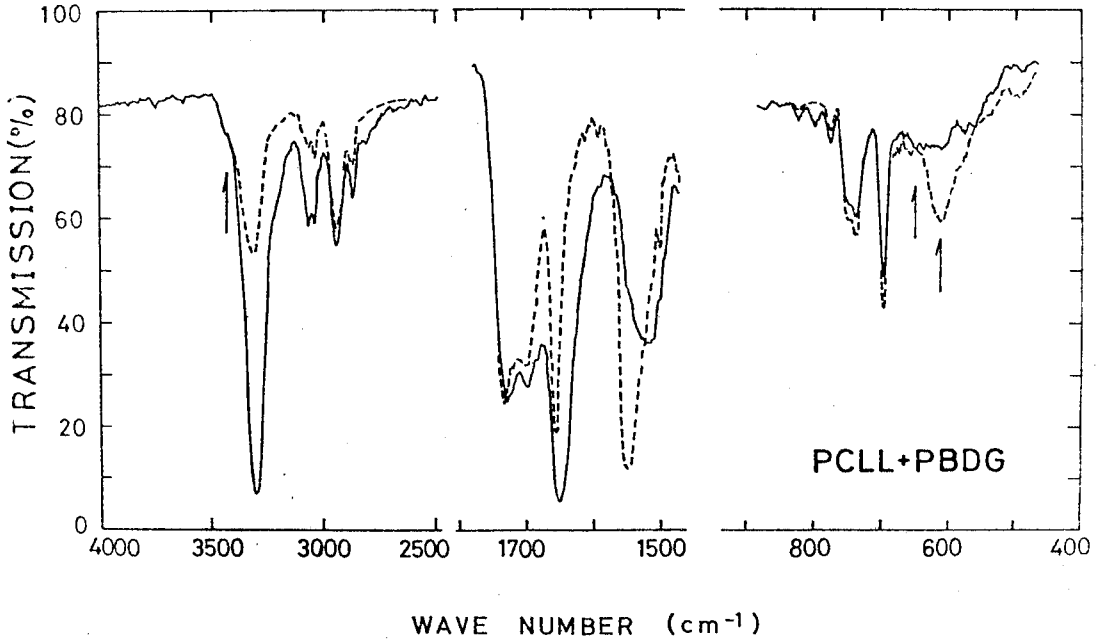

Figure 4.6 (c). Polarized infrared absorption spectrum of PCLBG: ------, electric vector perpendicular to the orientation direction; ———, electric vector parallel to the orientation direction.

to the N-carboxy amino(urethane) group of the side chain.

Figure 4.7 shows infrared absorption spectra of PCLBG at various temperatures from 23°C to 101°C. The free NH-stretching band at 3400 cm^{-1} becomes apparent with increasing temperature. Dielectric measurements showed that in this temperature range the side chain of PCLBG undergoes considerable motions while the main chain does not. Thus, the increase in intensity of free NH-stretching band seems to be related to the side-chain motion.

It is well known for polyamide and polyurethane that carboamide groups strongly interact through hydrogen bonds with neighboring molecules and that the networks of such hydrogen bonds play an important role in the physicochemical properties.[10] Hatano and Yoneyama reported that for poly(α-amino acid)s having a urethane group in the side chain, such as for PCLL, poly(δ-N-benzyloxycarbonyl-L-ornithine), and poly(γ-N-benzyloxycarbonyl-L-α,γ-diamino butyric acid), the urethane group is hydrogen bonded with those in the neighboring side chains in chloroform-dichloroacetic acid solution.[11] It is natural to consider that side chains of the polymers studied here are hydrogen bonded even in the solid state. Thus, the hydrogen-bonded NH-stretching absorption band at 3300 cm^{-1} is contributed from both the backbone and the side chain.

On the assumption that absorption coefficient of the NH-stretching vibrations at 3400 cm^{-1} is equal to that at 3300 cm^{-1}, the mole fraction of the hydrogen-bonded NH-group to all the urethane group of the side chain were estimated

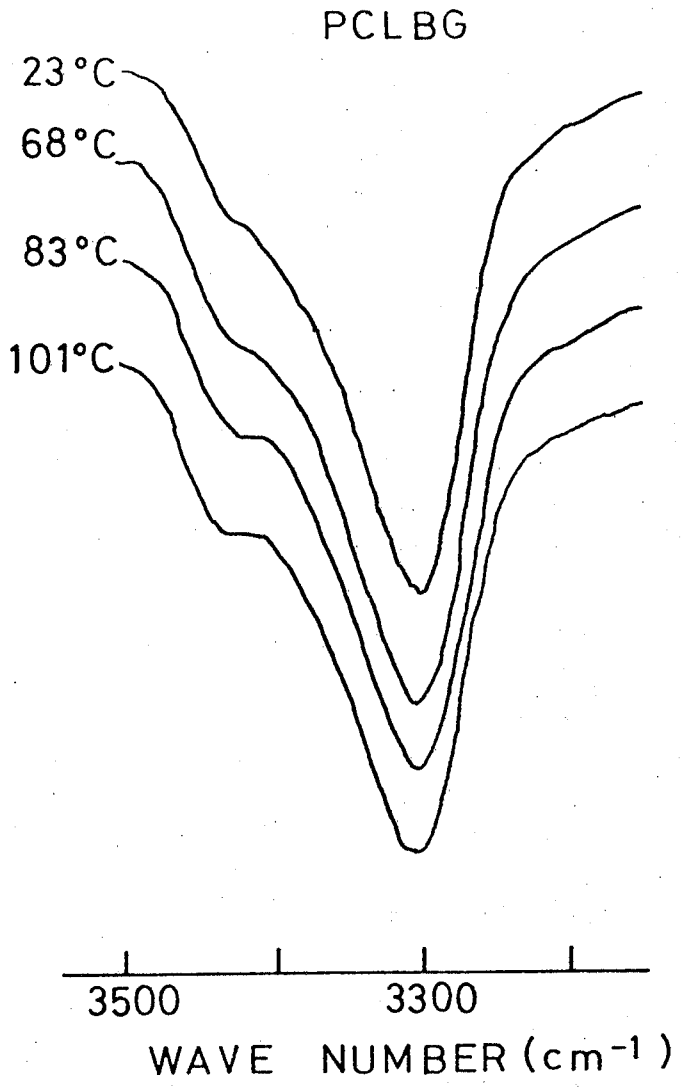

Figure 4.7. Infrared absorption spectra for PCLBG at indicated temperatures. The electric vector is perpendicular to the orientation direction.

to be 82, 61, and 19 %, for PCLL, PCLL + PBDG, and PCLBG, respectively.

Hatano and Yoneyama reported that the mole fraction of the hydrogen-bonded NH-groups for PCLL in chloroform-dichloroacetic acid solution is 38 %.[11] The mole fraction of the hydrogen-bonded NH-group in the solid state is much larger than in solution, beyond experimental error, suggesting that in the solid state a certain number of hydrogen bonds are formed between side chains of neighboring molecules. Furthermore, these results may imply that in the case of PCLL + PBDG, hydrogen bonds are possible between the urethane group in the side chain of the CLL-residue and the carbonyl group in the side chain of the BDG-residue.

When the polar urethane NH-group is hydrogen-bonded, side-chain motion will be so hindered that the dipole cannot be oriented to the applied electric field. Thus, the dielectric constant ε' observed will diminish upon increasing the mole fraction of hydrogen-bonded NH-groups.

As seen in Figure 4.1, the dielectric constant in the vicinity of room temperature for PCLL, PCLL + PBDG, and PCLBG are 3, 4, and 5, respectively. Thus, the mole fraction of hydrogen-bonded NH-group in the side chain expected from the dielectric constant ε' is in the order of PCLL > PCLL + PBDG > PCLBG.

This relation accords well with the relation among the mole fraction of hydrogen bonds estimated from infrared absorption spectra. The qualitative agreement of the frac-

tion of hydrogen bonds deduced by two independent methods enhances the reliability of the idea of the existence of hydrogen bonds in the side chain of PCLL in the solid state.

As noted in Table IV-1, the dielectric dispersion temperature was found to increase with increasing the fraction of hydrogen bonds. The higher dielectric-dispersion temperature of PCLL compared with those of PBLG and PMLG may be interpreted in terms of the hydrogen bonding of the side chains.

REFERENCES

1. Y. Yamashita, A. Tsutsumi, K. Hikichi, and M. Kaneko, Rep. Prog. Polym. Phys. Jpn., 18, 521 (1975).
2. Y. Yamashita, A. Tsutsumi, K. Hikichi, and M. Kaneko, Rep. Prog. Polym. Phys. Jpn., 19, 513 (1976).
3. N. Sasaki, A. Tsutsumi, K. Hikichi, and M. Kaneko, Rep. Prog. Polym. Phys. Jpn., 19, 521 (1976).
4. A. Tsutsumi, K. Hikichi, T. Takahashi, Y. Yamashita, N. Matsushima, M. Kanke, and M. Kaneko, J. Macromol. Sci.-Phys., B8, 413 (1973).
5. Y. Yamashita, A. Tsutsumi, K. Hikichi and M. Kaneko, Polym. J., 8, 114 (1975).
6. A. Tsutsumi, Jpn. J. Appl. Phys., 9, 2225 (1970).
7. A. Hiltner, J. M. Anderson, and E. Borkowski, Macromolecules, 5, 446 (1972).
8. K. Yamafuji, J. Phys. Soc. Jpn., 15, 2295 (1960).
9. R. Hayakawa and Y. Wada, J. Polym. Sci. Polym. Phys. Ed., 12, 2119 (1974).
10. N. G. McCrum, B. E. Read, and G. Williams, " Anelastic and Dielectric Effects in Polymer Solids," Wiley & Sons, London, 1967.
11. M. Hatano and M. Yoneyama, J. Am. Chem. Soc., 92, 1392 (1970).

CHAPTER V

DIELECTRIC PROPERTIES AND STRUCTURE OF COLLAGEN WITH ABSORBED WATER

Collagen is the most abundant protein in animals. It is an important component of supporting and connective tissues in biological system. Structure and properties of collagen and its absorption of water have been the significant subject of numerous studies.

The minimum unit of collagen is called " tropocollagen ". Tropocollagen is constructed by three similar but not identical peptide chains wound into a triple helix. It is a rod-like molecule about 2800 Å long and 10 Å diameter with a molecular weight of about 300,000. Tropocollagen molecules in function further aggregate to form higher level ordered structure, that is, " microfibril "," protofibril ", and " fibril ". Several protofibrils aggregate laterally to form fibrils with diameter up to several microns.

It has been widely accepted that the state of packing of tropocollagen is affected by the progress of the hydration. This implies that the collagen-water molecule interaction may play important roles in the assembly mechanism of tropocollagen in the native state.

In this chapter, the interaction of native collagen with water is investigated through the study of molecular motion using the method of dielectric measurements. The hydration process is pursued through the state of pack-

ing of tropocollagen by X-ray analysis.

V-1. EXPERIMENTAL

The collagen used in this study is from bovine Achilles tendons(BAT). The tendons were washed thoroughly with cold distilled water, and then immersed in dry acetone for a week to remove fat. BAT was cut into a rectangle 0.3 mm thick to make film for dielectric measurements. Conductive silver paste was painted on both surfaces as electrodes. The fiber axis of collagen is almost parallel to the electrodes.

The dielectric constant and loss factor were measured on an Ando Denki TR-10C bridge with a detector of Ando Denki BDA-9 and an Ando Denki WBG-9 oscillator. Measurements were made over a frequency range from 30Hz to 100kHz. The water fraction was changed from about 0.1 to 0.3(g water/g collagen). All measurements were performed at 20°C.

X-ray measurements were performed with a Rigaku Denki diffractometer using a scintillation counter with a pulse height analyzer and Ni-filtered Cu-K_α radiation. Wide-angle X-ray photographs were obtained with a flat-plate camera using Cu-K_α radiation. The incident beam is perpendicular to the film surface. Small-angle X-ray photographs were obtained with a flat camera at a specimen-to-film distance of 300 mm.

V-2. RESULTS

A. DIELECTRIC MEASUREMENTS

In Figure 5.1, the dielectric constant ε' of collagen with absorbed water is shown as a function of the volume fraction of water ϕ measured at various frequencies from 30Hz to 100kHz at room temperature. For all frequencies, ε' increases with increasing ϕ. At lower frequencies, the value of ε' becomes enormous to overgrow the value of pure water with increasing ϕ above a certain value. The region of ϕ where ε' rises appreciably depends on the measuring frequency; at higher frequency the increase of ε' begins at higher ϕ. These curves are qualitatively similar to the results presented by Rosen for various powdered proteins[1] and by Tomaselli and Shamos for native collagen.[2] They observed a sudden increase in the dielectric constant when water content increases above a certain value. They explained their data in terms of a transition in the hydration process, that is, the transition from the process of building up the monolayer of water molecules to that of thickening the crust of water around the protein. However, both of Rosen and Tomaselli and Shamos limited their measurements to a lower water content region than ours, and larger value of ε' than that of pure water was not observed. The behavior of ε' observed in the present study may be the characteristics of collagen-water system in a region of water content higher than that studied by

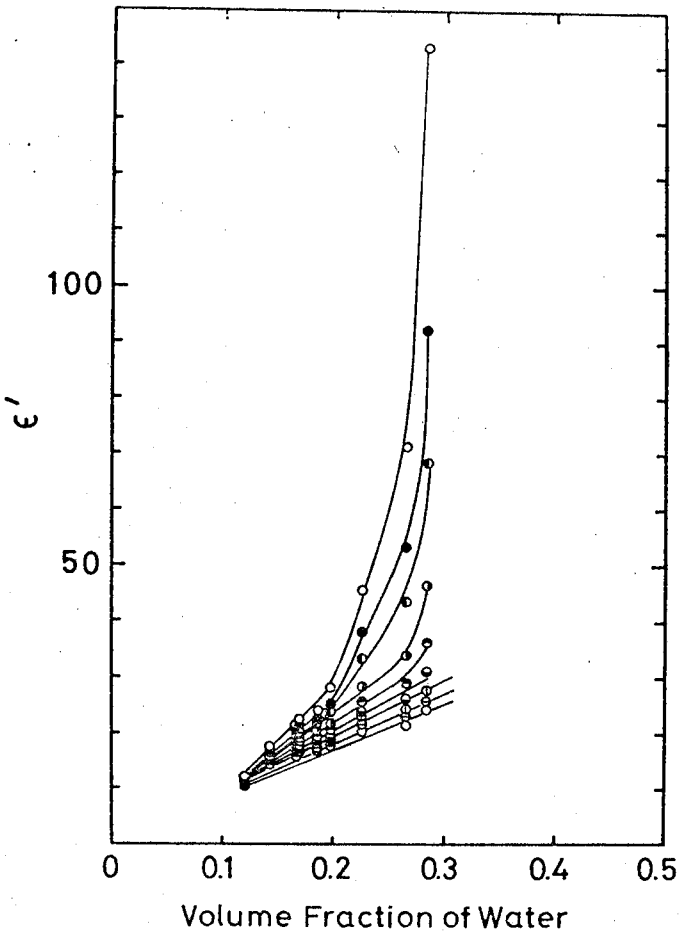

Figure 5.1. Hydration dependence of ε' measured at 30Hz(○), 60Hz(●), 110Hz(◐), 330Hz(◑), 1kHz(◓), 3kHz(◒), 10kHz(⦶), 30kHz(⊖), and 100kHz(○).

Tomaselli and Shamos.

Hoeve et al. observed the frequency dependence of ε' for hydrated collagen at a few different water contents.[3] They observed the considerably higher value of ε' at low frequencies in the same water content region as our experiments. In order to explain the enormous value of the dielectric constant, Hoeve et al. postulated a model of the water chain polarization on the basis of the results of NMR by Berendsen et al.[4] Taking their model into consideration, the frequency dependence of ε' in the water content region of rising of ε' observed in our experiments might be explained. However, because our dielectric measurements were done parallel to the fiber axis, not perpendicular as was the case of Hoeve et al., the water chain polarization model seems improbable.

B. ABSORPTION ISOTHERM AND BET PLOT

In order to obtain a clue for understanding the dielectric properties of collagen with absorbed water, it seems fruitful to pay regard to the molecular mechanism of hydration process of collagen. As for hydration of collagen, there have been numerous studies. It has been widely accepted that the absorption isotherm of native collagen in the low humidity region is well expressed by the Brunauer—Emett—Teller(BET) equation,[5]

$$w = \frac{w_0 \, c \, x}{(1 - x)[1 + (c - x)x]} \qquad (5.1)$$

where w represents the absorbed water measured in (g water/g collagen), w_0 is the amount of water of monolayer absorption, x represents the relative humidity, and c equals to $\exp[(E_1 - E_2)/ RT]$; E_1 being the heat of absorption of the first layer and E_2 that of higher order layer. In Figure 5.2 are shown the absorption isotherm and its BET plot of native collagen. In the BET plot, it is apparent that up to about 60 % relative humidity(about 0.25g water/g collagen) experimental points fit the linear relation of the BET theory. The value extrapolated to zero relative humidity in the BET plot, which represents the amount of water of monolayer absorption, was found to be about 0.1 g water/g collagen from our data for the bulk sample. This is comparable to that observed by Bull for powdered collagen.[6]

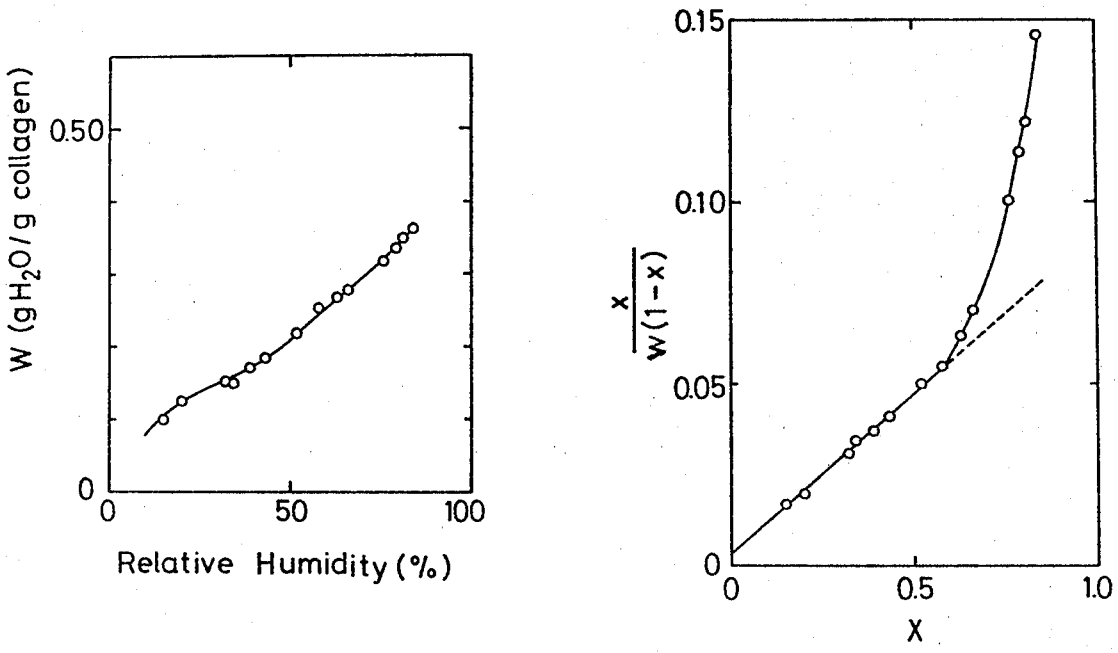

Figure 5.2. (a) Water absorption isotherm for BAT, and (b) the BET-plot of the isotherm.

C. X-RAY ANALYSIS

WIDE ANGLE X-RAY DIFFRACTION

In Figure 5.3, a typical wide-angle X-ray diffraction pattern of air dried BAT collagen is shown. The main features of the pattern are a strong meridional arc of a spacing of about 2.9 Å, discrete equatorial reflections of spacings of about 12 Å and 6 Å, and a diffuse equatorial blob of a spacing of about 4.5 Å. The spacing of 2.9 Å of a meridional reflection corresponds to the residual translation along the helical axis.

With respect to the lateral packing of tropocollagen, there have been two models: (1) Miller et al. proposed that four tropocollagens assemble to form a microfibril and the microfibrils pack on a tetragonal lattis.[7] (2) Woodhead-Galloway et al. introduced the concept of " planar liquid " to explain the lateral packing of tropocollagen.[8] In each model, the equatorial spacing of 12 Å has been considered to relate to the distance between neighboring tropocollagens. This equatorial reflection has been known to be sensitive to the absorbed water content.

In Figure 5.4, the spacing is plotted against the absorbed water content. The spacing increases with increasing water content, showing a skewed sigmoidal curve. Figure 5.5 shows the square of the spacing as plotted against water content. The square of the spacing is thought to be proportional to the volume of the inter-

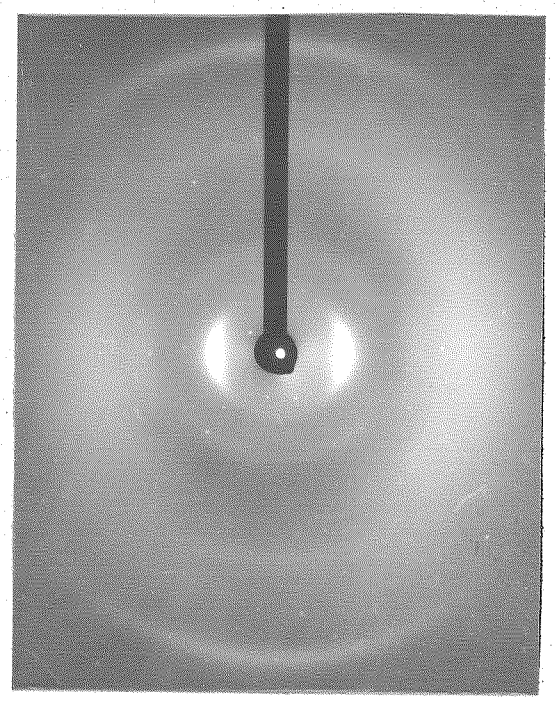

Figure 5.3. Wide-angle X-ray diffraction pattern of air dried BAT-collagen.

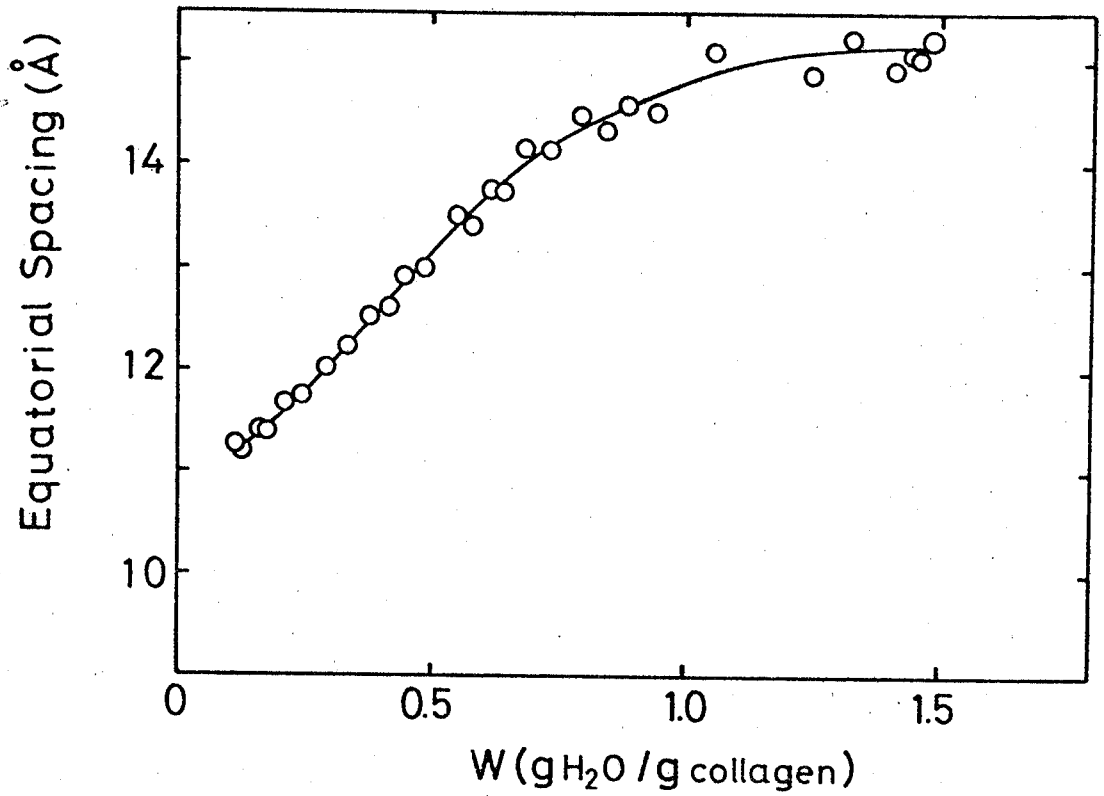

Figure 5.4. The spacing relating to the lateral packing of tropocollagen plotted against water content.

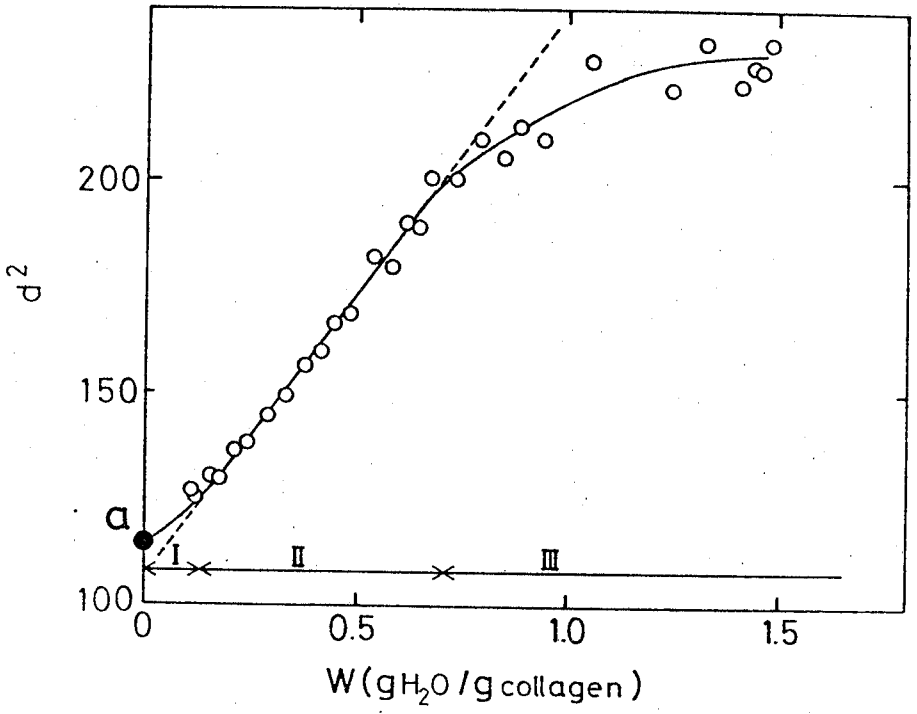

Figure 5.5. Square of the spacing plotted against water content.

a : The value for samples of thoroughly dried at room temperature. [M. A. Rougvie and R. S. Bear, J. Amer. Leather Chem. Ass., 48, 735 (1953).]

tropocollagen region, because the meridional 2.9 Å reflection does not change with the water content in the range studied. This figure shows that the hydration process of collagen can be divided into three stages. They are labelled stage I, stage II, and stage III in order of increasing hydration.

Stage I is the region of hydration corresponding to the absorbed water content up to 0.1g water/g collagen. In stage I the spacing is less sensitive to the absorbed water content compared with the case in stage II. The terminal point of stage I, about 0.1g water/g collagen, accords with the amount of water in the monolayer of the collagen absorption site, which was obtained from the BET plot in the preceding section. In this stage, water molecules occupy the absorption sites on inner-surfaces of collagen and build up monolayer.

Stage II is the region between the water content of 0.1 and 0.6g water/g collagen. In this stage the square of the spacing increases linearly with increasing water content. This suggests that in this region of hydration water molecules are accommodated into the inter-tropocollagen region. It seems that water molecules attach on the monolayer to thicken the crust of water layer in this stage.

Stage III is the region above 0.6g water/g collagen. In stage III, the spacing is less sensitive to the absorbed water content. The spacing at water contents more than 1g water/g collagen reaches to an asymptotic value of about 15 Å. A molecular mechanism of the hydration in stage III

should satisfy the conditions that the spacing does not increase remarkably though water molecules are further taken into the fibril.

SMALL ANGLE X-RAY DIFFRACTION

Figure 5.6 shows a small angle X-ray pattern of swollen collagen. Several meridional reflections are observed. On the equator a diffuse scattering is observed. Figure 5.7 shows a small angle X-ray pattern of air dried collagen. The diffuse scattering which is observed for swollen collagen is not observed. This diffuse scattering may be considered to be characteristic for stage III and may present some clue to the question where the water absorbed in stage III is stowed away. The diffuse scattering in Figure 5.6 seems to have characteristics which are reminiscent of commonly called " void scattering " of synthetic fibrous polymers.[9] The small angle X-ray pattern is examined for collagen swollen with ethylene glycol(Figure 5.8). The intensity is considerably diminished by soaking of ethylene glycol as compared with Figure 5.6. The intensity of the void scattering is proportional to the square of the difference in electron density between void and matrix. If we assume that the swelling reagent goes into void, the electron density difference between matrix and void will be greater for water than for ethylene glycol. The results indicated by Figures 5.6 and 5.8 support the above idea.

The swollen opaque corneal stroma has been known to consist of irregular regions or so-called " lakes ".[10] In these regions there exists no collagen at all and the size of the lake is comparable to the wave length of the visible ray, though seemed to have an appreciable distribution. Such irregularity has been considered to be origi-

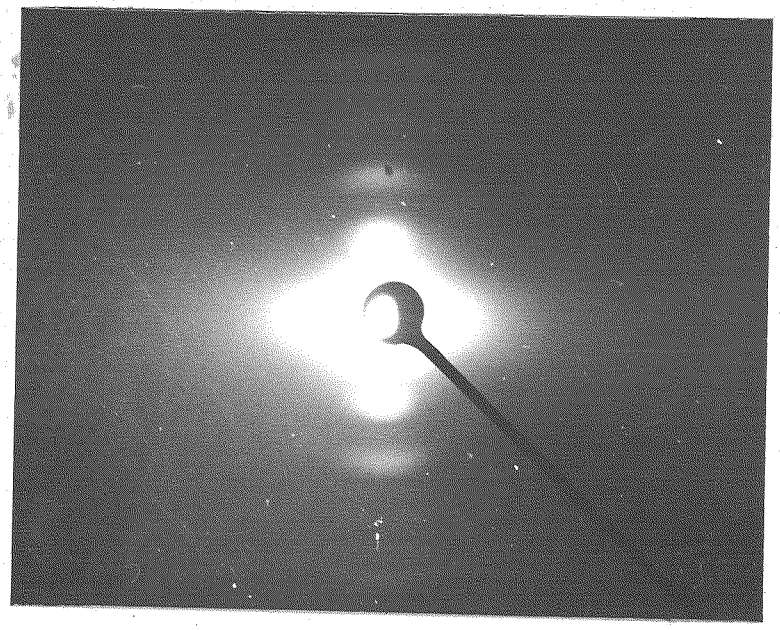

Figure 5.6. Small-angle X-ray pattern of swollen collagen.

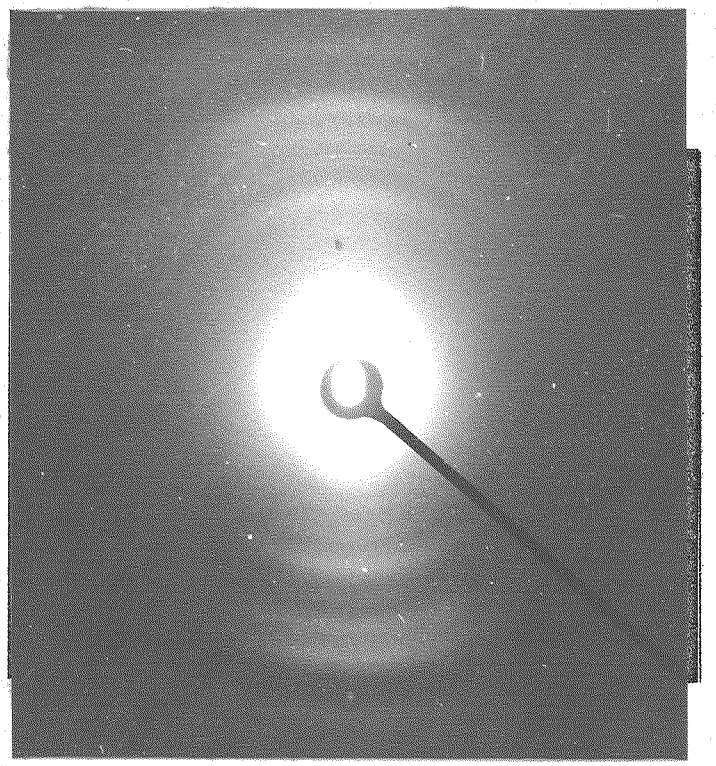

Figure 5.7. Small-angle X-ray pattern of air dried collagen.

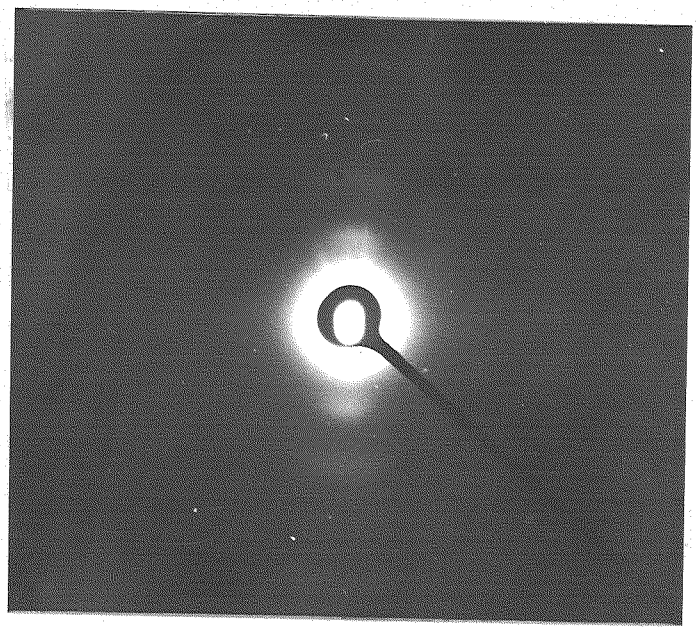

Figure 5.8. Small-angle X-ray pattern of collagen swollen with ethylene glycol.

nated from the remarkable localization of cross-links which increase with aging of collagen fibers. BAT from matured body must have a similar irregularity. The void-like region expected from the small angle X-ray pattern of the swollen collagen may be such a lake.

The water absorbed in stage III is impossible to enter the inter-tropocollagen region because of the cross-link, and may be considered to build up the pool of water molecules in collagen fiber.

V-3. DISCUSSION

In Figure 5.9, the division of hydration process presented in this study is compared with divisions by Nomura et al. and Pineri et al. which are based on the dynamic mechanical measurements and the thermal analysis, respectively.[11,12]

The correspondence of the three models of division shown in Figure 5.9 is as follows: (1) Stage I of our model corresponds to stage I of Nomura's and the region of stage I and stage II of Pineri's. (2) Stage II of ours covers the region of stage II and stage II' of Nomura's and the region of stage III and stage IV of Pineri's. (3) Though there is no exact agreement in the starting point of the final stage in each model, stage III of our model may be regarded to correspond to stage III of Nomura's and stage V of Pineri's.

The molecular mechanism of hydration in stage I deduced from our experiments accords with those of the corresponding division of Nomura et al. and Pineri et al. They termed waters building up monolayers tightly bound water.

Through stage II, the spacing between tropocollagens is found to increase linearly with the amount of water absorbed. On the basis of the structural studies stage II may be regarded as one stage hydration process. However, it is worth noting that both in Nomura's model and Pineri's model the corresponding process of hydration are futher divided into two stages. Indeed, our observation on molec-

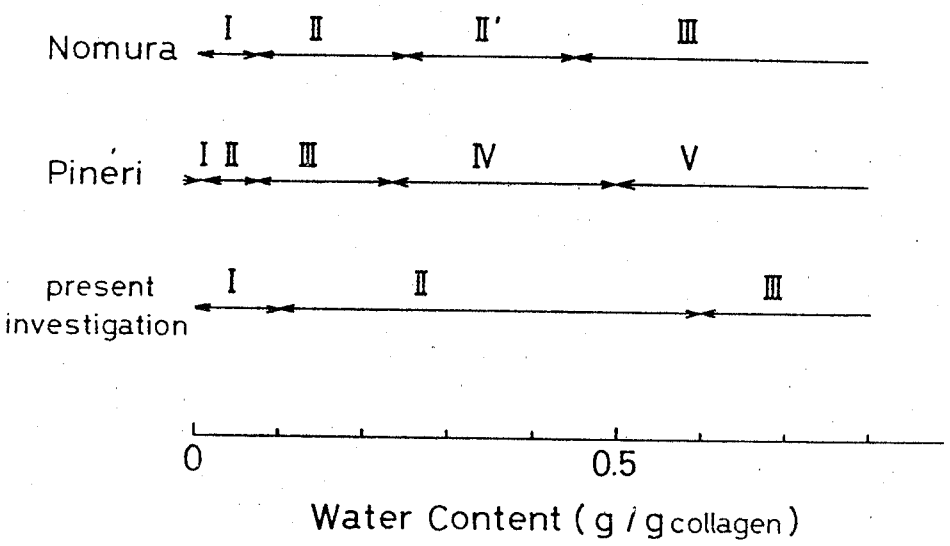

Figure 5.9. Comparison of the hydration process models.

ular motions of water-collagen system by dielectric measurements indicates two regions where ε' increases slowly and rapidly with water content.

It is of interest to note that stage II is one hydration process by structural studies while studies on molecular motions insist two processes. The change in molecular motions observed in stage II does not have any influence upon the structure.

Taking into consideration of these information on the structural transformation with the hydration, the dielectric properties of collagen with absorbed water are reconsidered.

Murphy and Lowry have explained the high dielectric constant of absorbent dielectrics in terms of the interstitial conduction in the crust of hydrated water of desorbed ions which were absorbed by dielectrics.[13] Collagen has some amount of ionizable amino acids. They may be deionized or neutralized by the attachment of the counter ions in the dry state. When such a system absorbs water and the crust of water surrounding each tropocollagen thickens to a proper amount of water, the counter ions may become free to move. High dielectric constant can be explained in terms of the polarization caused by the interstitial conduction of desorbed ions. According to this model, the water content region where the rapid rise of the dielectric constant occurs at each frequency may be attributed to the critical hydration where counter ions begin to move in a time scale of observation. This region was observed by

broad-line NMR measurements.[14]

REFERENCES

1. D. Rosen, Trans. Faraday Soc., 59, 2178 (1963).
2. V. P. Tomaselli and M. H. Shamos, Biopolymers, 12, 353 (1973).
3. C. A. J. Hoeve and P. C. Lue, Biopolymers, 13, 1661 (1974).
4. H. J. C. Berendsen, J. Chem. Phys., 36, 3297 (1962).
5. S. Brunauer, P. H. Emmett, and E. Teller, J. Am. Chem. Soc., 60, 309 (1938).
6. H. B. Bull, J. Am. Chem. Soc., 66, 1499 (1944).
7. A. Miller and D. A. D. Parry, J. Mol. Biol., 75, 441 (1973).
8. J. Woodhead-Galloway and P. A. Machin, Acta Cryst., A 32, 368 (1976).
9. W. O. Statton, J. Polym. Sci., 22, 385 (1956).
10. G. B. Benedek, Appl. Opt., 10, 459 (1971).
11. S. Nomura, A. Hiltner, J. B. Lando, and E. Baer, Biopolymers, 16, 231 (1977).
12. M. H. Pineri, M. Escoubes, and G. Roche, Biopolymers, 17, 2799 (1978).
13. E. J. Murphy and H. H. Lowry, J. Phys. Chem., 34, 598 (1930).
14. S. Kazama, unpublished results.

Chapter VI

CONCLUSION

The decrease in breadth of the distribution of the dielectric relaxation time with the increase in the side-chain length of PnALG provides an evidence of the validity of the two-phase model for poly(α-amino acid) in the solid state. This suggests that interactions occurring in poly-(α-amino acid) are divided into the side chain—backbone and the side chain—side chain interactions.

The dielectric dispersion of monosubstituted PBDG indicates that substituents introduced to the phenyl ring of the side chain brings about strong influence upon side-chain motions. This influence is most remarkable for p-substitution in three monochloro-PBDGs and can be explained mainly in terms of the dipole—dipole interactions among the " exposed " C—Cl dipoles of p-ClPBDG. The restriction upon side-chain motions is enhanced by the increase in polarity and bulkiness of the substituent. For o-Cl PBDG, a steric hinderance between the o-Cl and the carboxy group determines a side-chain conformation which gives the large resultant dipole moment. For a racemic mixture of p-ClPBDG and p-ClPBLG, no evidence of phenyl ring stacks of the side chain was observed, although such stacks are believed to exist for PBDG + PBLG.

The high dispersion temperatures observed for PCLL, PCLL + PBDG, and PCLBG as compared with those of PBLG and

PMLG imply the existence of a strong interaction in these polymers. Infrared absorption spectra revealed that there are hydrogen bonds among urethane groups of the CLL-side chains. The order of the dielectric constant ε' in the vicinity of room temperature, PCLL(3) < PCLL + PBDG(4) < PCLBG(5) was well explained in terms of hydrogen bonds in the side chains of these polymers studied by infrared absorption spectra. The dispersion temperatures were also found to be related to the fraction of hydrogen bonds. The existence of hydrogen bonds in the side chain was found to be one of the important factors in understanding the properties of PCLL and the related poly(α-amino acid)s in the solid state.

The hydration process of collagen was divided into three parts. Stage I of the hydration is the process where water molecules occupy the absorption sites on inner-surfaces of collagen to build up monolayer. In stage II, water molecules attach on monolayer to thicken the crust of water layer. In hydration stage III, the water absorbed is considered to build up the pool of the water molecules in collagen fiber.

The dielectric constant increases rapidly to the enormous value in stage II. This was explained in terms of the polarization due to the interstitial conduction of desorbed ions in the thickening crust of water surrounding tropocollagen.